

RESEARCH ARTICLE

Type 3 secretion system induced leukotriene B4 synthesis by leukocytes is actively inhibited by *Yersinia pestis* to evade early immune recognition

Amanda Brady¹, Katelyn R. Sheneman¹, Amanda R. Pulsifer^{1^{aa}}, Sarah L. Price^{1^{ab}}, Taylor M. Garrison¹, Krishna Rao Maddipati², Sobha R. Bodduluri¹, Jianmin Pan^{3^{ac}}, Nolan L. Boyd⁴, Jing-Juan Zheng⁴, Shesh N. Rai^{5^{ac}}, Jason Hellmann⁴, Bodduluri Haribabu¹, Silvia M. Uriarte⁶, Matthew B. Lawrenz^{1,7*}

1 Department of Microbiology and Immunology, University of Louisville School of Medicine, Louisville, Kentucky, United States of America, **2** Department of Pathology, Lipidomics Core Facility, Wayne State University, Detroit, Michigan, United States of America, **3** Biostatistics and Bioinformatics Facility, Brown Cancer Center, University of Louisville, Louisville, Kentucky, United States of America, **4** Center for Cardiometabolic Science, Christina Lee Brown Environment Institute, Division of Environmental Medicine, University of Louisville School of Medicine, Louisville, Kentucky, United States of America, **5** Department of Pharmacology and Toxicology, University of Louisville School of Medicine, Louisville, Kentucky, United States of America, **6** Department of Oral Immunology & Infectious Diseases, University of Louisville, Louisville, Kentucky, United States of America, **7** Center for Predictive Medicine for Biodefense and Emerging Infectious Diseases, Louisville, Kentucky, United States of America

^{aa} Current address: StemCell Technologies, Vancouver, Canada

^{ab} Current address: Vanderbilt University, Nashville, Tennessee, United States of America

^{ac} Current address: University of Cincinnati, Cincinnati, United States of America

* matt.lawrenz@louisville.edu



OPEN ACCESS

Citation: Brady A, Sheneman KR, Pulsifer AR, Price SL, Garrison TM, Maddipati KR, et al. (2024) Type 3 secretion system induced leukotriene B4 synthesis by leukocytes is actively inhibited by *Yersinia pestis* to evade early immune recognition. PLoS Pathog 20(1): e1011280. <https://doi.org/10.1371/journal.ppat.1011280>

Editor: Joan Meccas, Tufts University, UNITED STATES

Received: March 12, 2023

Accepted: January 16, 2024

Published: January 25, 2024

Copyright: © 2024 Brady et al. This is an open access article distributed under the terms of the [Creative Commons Attribution License](https://creativecommons.org/licenses/by/4.0/), which permits unrestricted use, distribution, and reproduction in any medium, provided the original author and source are credited.

Data Availability Statement: All relevant data are within the manuscript and its [Supporting Information](#) files.

Funding: This work was supported by funding from the National Institutes of Health NIAID T32AI132146 (AB), NIAID F31AI178999 (KRS), NIAID F31AI147404 (SLP), NIAID R01AI148241-S2 (TMG), NIGMS GM127495 (JH), NIGMS GM127607 (JH), NIAID R01AI148241 (MBL), NIAID R01AI178106 (MBL), NIGMS

Abstract

Subverting the host immune response to inhibit inflammation is a key virulence strategy of *Yersinia pestis*. The inflammatory cascade is tightly controlled via the sequential action of lipid and protein mediators of inflammation. Because delayed inflammation is essential for *Y. pestis* to cause lethal infection, defining the *Y. pestis* mechanisms to manipulate the inflammatory cascade is necessary to understand this pathogen's virulence. While previous studies have established that *Y. pestis* actively inhibits the expression of host proteins that mediate inflammation, there is currently a gap in our understanding of the inflammatory lipid mediator response during plague. Here we used the murine model to define the kinetics of the synthesis of leukotriene B4 (LTB₄), a pro-inflammatory lipid chemoattractant and immune cell activator, within the lungs during pneumonic plague. Furthermore, we demonstrated that exogenous administration of LTB₄ prior to infection limited bacterial proliferation, suggesting that the absence of LTB₄ synthesis during plague contributes to *Y. pestis* immune evasion. Using primary leukocytes from mice and humans further revealed that *Y. pestis* actively inhibits the synthesis of LTB₄. Finally, using *Y. pestis* mutants in the Ysc type 3 secretion system (T3SS) and *Yersinia* outer protein (Yop) effectors, we demonstrate that leukocytes recognize the T3SS to initiate the rapid synthesis of LTB₄. However, several Yop effectors secreted through the T3SS effectively inhibit this host response. Together, these data demonstrate that *Y. pestis* actively inhibits the synthesis of the inflammatory lipid LTB₄

P20GM125504 (MBL), and in part from the Jewish Heritage Foundation for Excellence Grant Program at the University of Louisville School of Medicine (MBL). Lipidomic analysis was supported in part by National Center for Research Resources, National Institutes of Health Grant S10RR027926 (KRM). The funders had no role in study design, data collection and analysis, decision to publish, or preparation of the manuscript.

Competing interests: The authors have declared that no competing interests exist.

contributing to the delay in the inflammatory cascade required for rapid recruitment of leukocytes to sites of infection.

Author summary

Yersinia pestis targets the host's innate immune response to inhibit inflammation. Because the generation of a non-inflammatory environment is required for infection, defining the mechanisms used by *Y. pestis* to block inflammation is key to understanding its virulence. Lipid mediators are potent signaling molecules required for timely initiation of host inflammation. While previous studies have demonstrated that *Y. pestis* inhibits inflammation, there is a gap in our understanding of the inflammatory lipid mediator response during plague. Here we show that *Y. pestis* inhibits the production of one of these critical lipid mediators, leukotriene B4, by host immune cells. Furthermore, we identify both the signals that induce LTB₄ production by leukocytes and the mechanisms used by *Y. pestis* to inhibit this process. Together, these data represent the first comprehensive analysis of inflammatory lipids produced during pneumonic plague and improve our current understanding of how *Y. pestis* manipulates the host immune response to generate a permissive non-inflammatory environment required to colonize the mammalian host.

Introduction

Yersinia pestis causes the human disease known as the plague. Although typically characterized as a disease of our past, in the aftermath of the 3rd plague pandemic, *Y. pestis* became endemic in rodent populations in several countries, increasing the potential for spillover into human populations through contact with infected animals and fleas [1–3]. Human plague manifests in three forms: bubonic, septicemic, or pneumonic plague. Bubonic plague resulting from flea transmission arises when bacteria colonize and replicate within lymph nodes. Septicemic plague results when *Y. pestis* gains access to the bloodstream, either directly from a flea bite or via dissemination from an infected lymph node, and results in uncontrolled bacterial replication and sepsis. Finally, secondary pneumonic plague, wherein *Y. pestis* disseminates to the lungs via the blood, results in a pneumonia that can promote direct person-to-person transmission via aerosols. While treatable with antibiotics, if left untreated, all forms of plague are associated with high mortality rates, and the probability of successful treatment decreases the longer initiation of treatment is delayed post-exposure [3–6]. Regardless of the route of infection, one of the key virulence determinants for *Y. pestis* to colonize the host is the Ysc type 3 secretion system (T3SS) encoded on the pCD1 plasmid [5,7]. This secretion system allows direct translocation of bacterial effector proteins, called Yops, into host cells [5,8,9]. The Yop effectors target specific host factors to disrupt normal host cell signaling pathways and functions [10–15]. Because the T3SS and Yops are required for mammalian but not flea infection, the expression of the genes encoding these virulence factors are differentially expressed within these two hosts [5,8,16,17]. The primary signal leading to T3SS and Yop expression is a shift in temperature from that of the flea vector (<28°C) to that of the mammalian host (>30°C). During mammalian infection, *Y. pestis* primarily targets neutrophils and macrophages for T3SS-mediated injection of the Yop effectors [18–20]. The outcomes of Yop injection into these cells include inhibition of phagocytosis, reactive oxygen species (ROS) synthesis, degranulation by neutrophils, and inflammatory cytokine and chemokine release required to recruit circulating

neutrophils to infection sites [21–26]. Importantly, previous work suggests that inhibition of neutrophil influx and establishing a non-inflammatory environment is crucial for *Y. pestis* virulence [27,28]. Therefore, defining the molecular mechanisms used by *Y. pestis* to subvert the host immune response is fundamental to understanding the pathogenesis of this organism. Moreover, defining the host mechanisms targeted by *Y. pestis* to inhibit inflammation can also provide novel insights into how the host responds to bacterial pathogens to control infection.

A cascade of events tightly regulates inflammation to ensure rapid responses to control infection and effective immune resolution after clearance of pathogens to limit tissue damage [29,30]. This inflammatory cascade is initiated by synthesizing potent lipid mediators and is sustained and amplified by the subsequent production of protein mediators [31,32]. Polyunsaturated fatty acid (PUFA)-derived lipid mediators are potent modulators of the innate and adaptive immune responses [30,33]. Of these, the eicosanoids, including the leukotrienes and the prostaglandins, are key regulators of the inflammatory cascade during infection [31,32]. Leukotriene B4 (LTB₄) is rapidly synthesized from arachidonic acid upon activation of 5-lipoxygenase (5-LOX), cytosolic phospholipase A₂ (cPLA₂), 5-LOX activating protein (FLAP), and LTA₄ hydrolase (Fig 1A) [34]. Upon synthesis and release, LTB₄ is recognized by the high affinity BLT1 receptor on immune cells to promote chemotaxis and initiate the inflammatory cascade leading to production of pro-inflammatory cytokines and chemokines [31,32,35–39]. Together these inflammatory mediators promote the recruitment of circulating leukocytes to infected tissue [32]. Importantly, because of its critical role in initiating the inflammatory cascade, disruption in the timely production of LTB₄ can slow the subsequent downstream release of cytokines and chemokines and the ability of the host to mount a rapid inflammatory response required to control infection.

Despite active proliferation of *Y. pestis* within the lungs in the mouse model, there appears to be an absence of pro-inflammatory cytokines, chemokines, and neutrophil influx for the first 36 hours of primary pneumonic plague [11–15]. This phenotype dramatically differs from pulmonary infection with attenuated mutants of *Y. pestis* lacking the T3SS or Yop effectors or by other pulmonary pathogens, such as *Klebsiella pneumoniae*, which induce significant inflammation within 24 hours of bacterial exposure [11–15]. Surprisingly, despite the importance of lipid mediators in initiating the inflammatory cascade, the role of inflammatory lipids during plague has not been previously investigated. However, using human peripheral blood neutrophils, Pulsifer et al. previously demonstrated that *Y. pestis* can actively inhibit the synthesis of LTB₄ *in vitro* in a T3SS/Yop-dependent manner, suggesting that LTB₄ synthesis may be inhibited during plague [26]. In this study, we expand on these observations by investigating LTB₄ synthesis by the mammalian host in response to *Y. pestis*. Using the murine model of plague, we demonstrate dysregulation in the production of LTB₄ by *Y. pestis* and provide the lipidomic profile of other host inflammatory lipids during the initial 48 h of pneumonic plague. We further show that exogenous treatment with LTB₄ inhibits bacterial proliferation in the murine model. Using *Y. pestis* mutants, we also discovered that leukocyte interactions with the *Y. pestis* T3SS triggers LTB₄ synthesis, but synthesis is inhibited by multiple Yop effectors secreted via the same T3SS. Together, these data suggest that modulation in the production of host inflammatory lipids is an additional virulence mechanism used by *Y. pestis* to inhibit the rapid recruitment of immune cells needed to control infection.

Results

LTB₄ synthesis is delayed during pneumonic plague

Based on our previous observations that *Y. pestis* inhibits LTB₄ synthesis by human neutrophils [26], we sought to determine if LTB₄ was synthesized during infection using the murine

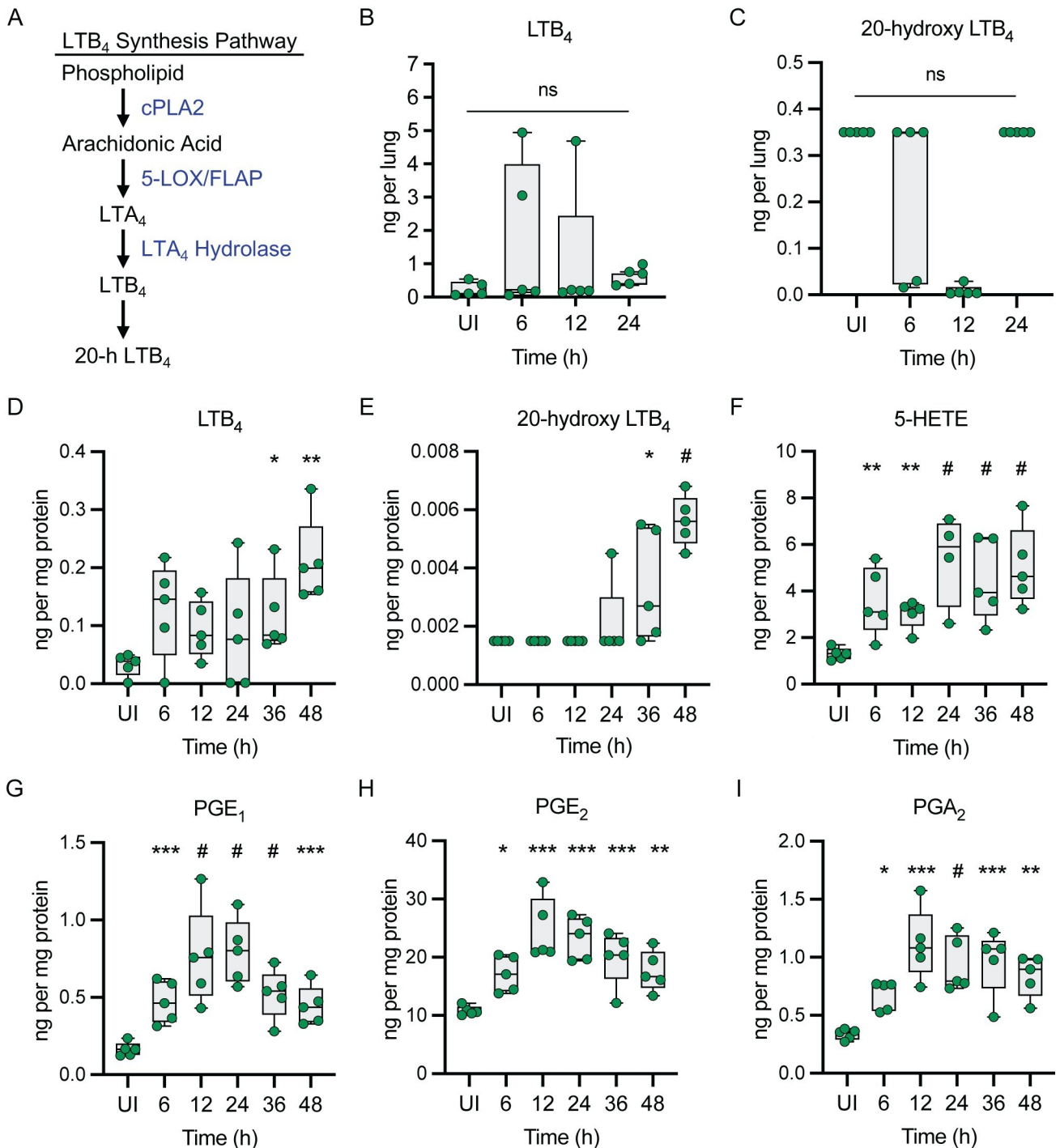


Fig 1. LTB₄ synthesis is blunted during pneumonic plague. (A) The LTB₄ synthesis pathway. (B-I) C56BL/6J mice were infected with 10 x the LD₅₀ *Y. pestis* KIM5+ and lungs were harvested at the indicated times (n = 5) to measure host lipids by LC-MS. UI = samples from uninfected animals. (B) LTB₄ concentrations. (C) 20-hydroxy LTB₄ concentrations. (D) LTB₄ concentrations. (E) 20-hydroxy LTB₄ concentrations. (F) 5-HETE concentrations. (G) PGE₁ concentrations. (H) PGE₂ concentrations. (I) PGA₂ concentrations. Each symbol represents an individual mouse and the box plot represents the median of the group ± the range. Changes in lipid concentrations were compared to the UI sample using (B-C) One-way ANOVA with Dunnett's *post hoc* test or (D-I) the LIMMA—Moderated t-test. ns = not significant, * = p ≤ 0.05, ** = p ≤ 0.01, *** = p ≤ 0.001, # = p ≤ 0.0001.

<https://doi.org/10.1371/journal.ppat.1011280.g001>

model of pneumonic plague. C57BL/6J mice were intranasally infected with *Y. pestis* KIM5+ and LTB₄ was measured in the lungs during the non-inflammatory stage of disease (6, 12, and 24 h post-infection). We did not observe a statistically significant increase in LTB₄ synthesis at any time point, with only 3 of the 15 samples having elevated LTB₄ concentrations over the entire 24 h period (Fig 1B). Moreover, we did not observe a significant increase in 20-hydroxy LTB₄ (Fig 1C), which is the direct degradation product of LTB₄ (Fig 1A). To confirm these results, LTB₄ was measured in the lungs from a second independent group of C57BL/6J mice, this time expanding the analysis to include the pro-inflammatory stage of disease (36 and 48 h post-infection). Again, we did not observe statistically significant increases in LTB₄ or 20-hydroxy LTB₄ during the first 24 h of infection (Fig 1D and 1E). However, by 36 h post-infection, both lipids were statistically elevated compared to uninfected samples ($p \leq 0.05$). Moreover, we observed a significant increase in 5-HETE as early as 6 h post-infection (Fig 1F; $p \leq 0.01$), which can result if 5-LOX does not complete the synthesis of LTA₄ from arachidonic acid [40,41]. While the synthesis of LTB₄ appears absent during the first 24 h of infection, the synthesis of other inflammatory lipids increased during the same period, including the prostaglandins, which are another group of eicosanoids whose synthesis is regulated via the cyclooxygenase pathway (Fig 1G–1I). Globally, we observed significant changes in the synthesis of 63 lipids during pneumonic plague, including lipids generally considered to be pro-inflammatory (18 lipids), anti-inflammatory (41 lipids), or pro-resolving (4 lipids) (S1 Table) [42,43]. Together these data indicate LTB₄ synthesis is delayed during pneumonic plague.

BLT1^{-/-} mice are not more susceptible to pneumonic plague than C57BL/6J mice

LTB₄ is recognized by the high-affinity G-protein coupled receptor BLT1, which is expressed primarily by innate and adaptive immune cells [38,44]. LTB₄-BLT1 engagement leads to host inflammatory immune responses such as chemotaxis, cytokine release, phagocytosis, and ROS production that contribute to the clearance of pathogens [35,45]. Mice deficient in the expression of BLT1 cannot effectively respond to LTB₄ signaling and are generally more susceptible to infection [39,46,47]. Because we did not observe LTB₄ synthesis during the early stages of pneumonic plague, we hypothesized that BLT1^{-/-} mice would not be more susceptible to *Y. pestis* infection. To test this hypothesis, we intranasally infected C57BL/6J and BLT1^{-/-} mice with *Y. pestis* KIM5+ and measured bacterial numbers in the lungs at 12 and 24 h post-infection. Bacterial numbers were not significantly higher in BLT1^{-/-} mice than C57BL/6J mice (Fig 2A). Furthermore, independent experiments with a *Y. pestis* strain with a luciferase bioreporter (*Y. pestis* CO92 Lux_{p_{cysZK}}), which allows for monitoring bacterial proliferation via optical imaging and host survival in the same group [48], showed no significant differences between the two mouse lines in bacterial proliferation at later time points or in the mean-time to death (Fig 2B and 2C). These data indicate that the loss of LTB₄-BLT1 signaling in BLT1^{-/-} mice does not impact the infectivity of *Y. pestis*, further supporting that LTB₄ synthesis and signaling is disrupted during pneumonic plague.

Exogenous LTB₄ treatment limits *Y. pestis* proliferation *in vivo*

Because LTB₄ synthesis and signaling appears to be disrupted during infection, we next asked if exogenous administration of LTB₄ could alter infection. To test this hypothesis, we used a previously described peritoneal model that allows for accurate administration of LTB₄ and easy recovery of both elicited leukocytes and bacteria via lavage [49]. As described previously, intraperitoneal administration of LTB₄ resulted in an increase in the neutrophil population

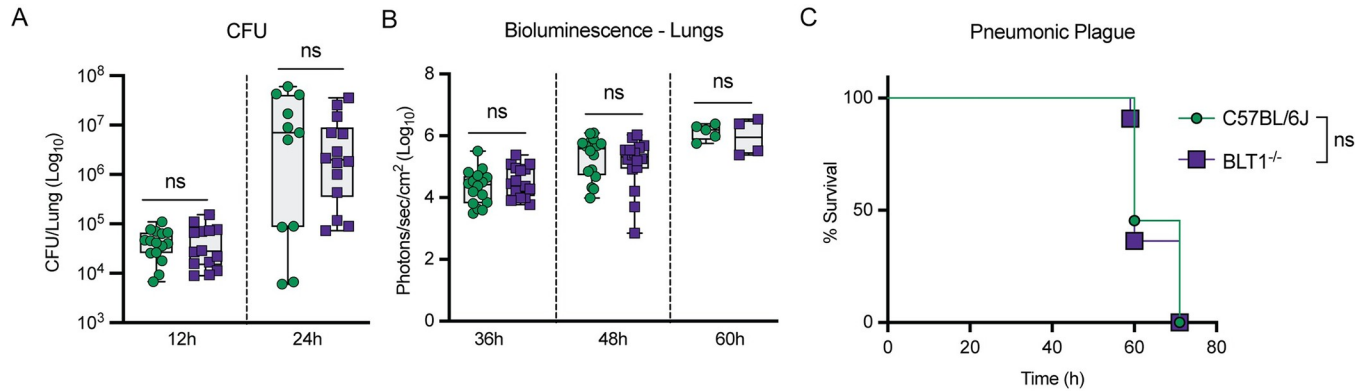


Fig 2. BLT1^{-/-} mice are not more susceptible to pneumonic plague than C57BL/6J mice. (A) C57BL/6J (green circles) or BLT1^{-/-} (purple squares) mice were infected intranasally with 10 x the LD₅₀ of *Y. pestis* KIM5+ and lungs were harvested at 12 and 24 h post-infection. Bacterial proliferation within the lungs was determined by CFU enumeration. Each symbol represents an individual mouse and the box plot represents the median of the group ± the range. Combined data from two independent experiments. (B-C) C57BL/6J (green circles) or BLT1^{-/-} (purple squares) mice were infected intranasally with 10x the LD₅₀ of *Y. pestis* CO92 LUX_{p_{cy}sZK}. (B) Bacterial proliferation in the lungs as a function of bioluminescence. Each symbol represents an individual mouse and the box plot represents the median of the group ± the range. Combined data from two independent experiments. (C) Survival curves of mice from B (n = 15). For A and B, T-test with Mann-Whitney's *post hoc* test indicated no statistically significant (ns) differences between C57BL/6J and BLT1^{-/-} groups. For C, Log-Rank analysis revealed no statistically significant (ns) differences in survival between the two groups.

<https://doi.org/10.1371/journal.ppat.1011280.g002>

within the peritoneal cavity in C57BL/6J mice as early as 1 h post-administration (Figs 3A and S1) [49]. When challenged intraperitoneally with *Y. pestis* KIM5+ after LTB₄ administration, we observed a significant decrease in the number of viable bacteria recovered from LTB₄-treated animals, approaching the limit of detection, as compared to PBS-treated animals 3 h

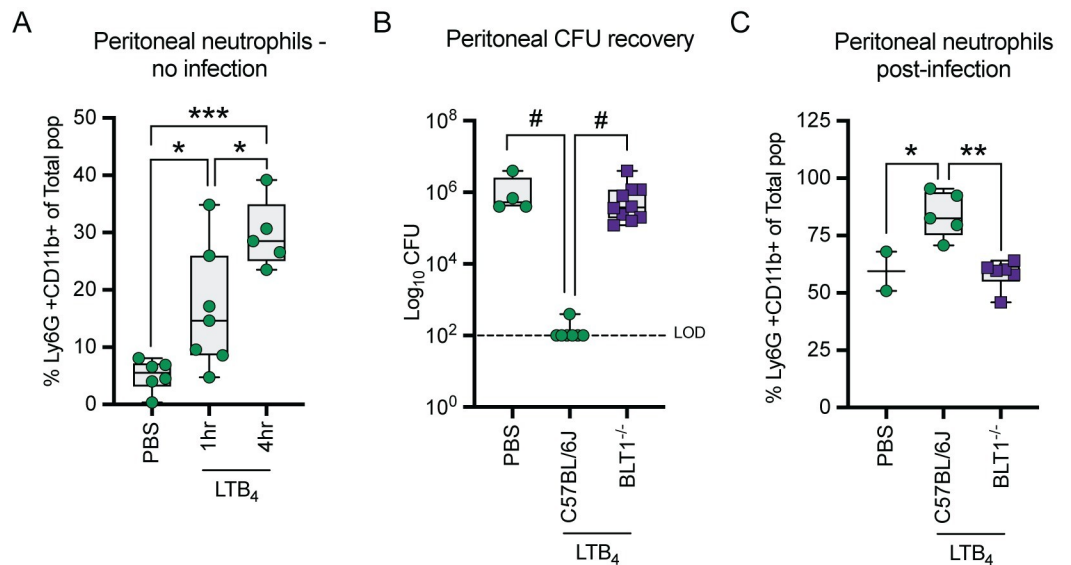


Fig 3. LTB₄ treatment improves host killing of *Y. pestis*. (A) C57BL/6J mice administered 1 x DPBS (PBS) or 10 nmol LTB₄ intraperitoneally and changes in neutrophil populations (Ly6G+CD11b⁺) were measured at 1 or 4 h post-treatment. (B) C57BL/6J (green circles) or BLT1^{-/-} (purple squares) mice administered DPBS or 10 nmol LTB₄ were infected 1 h later with 10⁵ CFU of *Y. pestis* KIM5+ and bacterial numbers in the peritoneal cavities were enumerated 3 h post-inoculation. LOD = Limit of detection. (C) Neutrophil populations from a subset of animals from B. Each symbol represents an individual mouse and the box plot represents the median of the group ± the range. Combined data from three independent experiments. One-way ANOVA with Tukey's *post hoc* test compared to each condition. * = p ≤ 0.05, ** = p ≤ 0.01, *** = p ≤ 0.001, # = p ≤ 0.0001.

<https://doi.org/10.1371/journal.ppat.1011280.g003>

post-infection (Fig 3B; $p \leq 0.0001$). Neutrophil numbers also remained significantly elevated in the LTB_4 -treated animals at 3 h post-infection compared to PBS-treated animals (Fig 3C; $p \leq 0.05$). Moreover, bacterial clearance was dependent on LTB_4 signaling, as LTB_4 treatment of $BLT1^{-/-}$ mice did not alter bacterial or neutrophil numbers at 3 h post-infection compared to PBS-treated C57BL/6J mice (Fig 3B and 3C). Together, these data indicate that LTB_4 -mediated recruitment and activation of leukocytes can improve the host response to *Y. pestis*.

Neutrophils do not synthesize LTB_4 in response to *Y. pestis*

Because neutrophils are robust sources of LTB_4 [35], are the primary cells with which *Y. pestis* interacts during the first 24 h of pneumonic plague [19], and *Y. pestis* inhibits LTB_4 synthesis by human neutrophils [26], we next sought to determine if the LTB_4 response by neutrophils differed between *Y. pestis* and other bacteria. When bone marrow-derived neutrophils (BMNs) from C57BL/6J mice were stimulated with *E. coli*, *S. enterica* Typhimurium, or a *K. pneumoniae manC* mutant (unable to synthesize a capsule), LTB_4 synthesis was significantly induced within 1 h of infection (Fig 4A; $p \leq 0.0001$). However, infection with *Y. pestis* did not elicit LTB_4 synthesis, even when the MOI was increased to 100 bacteria per neutrophil (Fig 4B). Similar phenotypes were observed during infection of human peripheral blood neutrophils (hPMNs), recapitulating our previously published data for *Y. pestis* (Fig 4C and 4D) [26]. Importantly, the absence of LTB_4 synthesis did not appear to be due to *Y. pestis* induced cell death, as no significant changes in cell permeability or cytotoxicity were observed during *Y. pestis* infections at an MOI of 20 when compared to uninfected neutrophils (S2A and S2B Fig). Even at an MOI of 100, while cell permeability appeared slightly elevated in *Y. pestis*-infected murine neutrophils compared to uninfected cells (S2C Fig; 9% vs. 28%), overall cytotoxicity was lower in *Y. pestis*-infected cells (S2D Fig; 12% vs. 4%). Similarly, *Y. pestis* did not induce elevated permeability or cytotoxicity in human neutrophils (S2E and S2F Fig). These data demonstrate that while neutrophils can rapidly synthesize LTB_4 in response to other bacterial pathogens, neither murine nor human neutrophils appear to synthesize LTB_4 in response to *Y. pestis*.

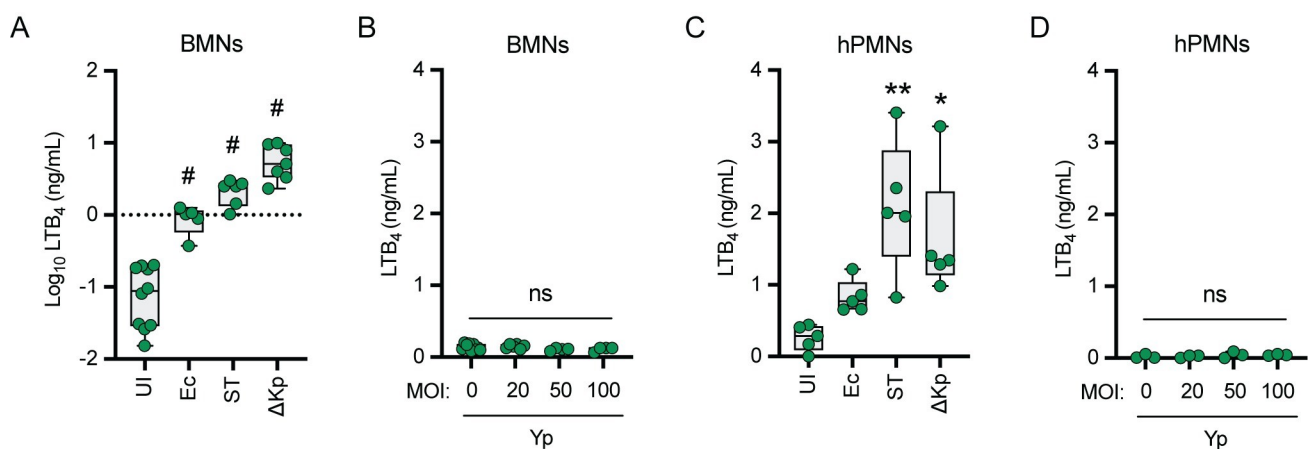


Fig 4. Neutrophils do not synthesize LTB_4 in response to *Y. pestis*. (A–B) Murine (BMNs) or (C–D) human (hPMNs) neutrophils were infected with *E. coli* DH5 α (Ec), *S. enterica* Typhimurium LT2 (ST), or *K. pneumoniae manC* (Δ Kp) at an MOI of 20, or with *Y. pestis* (Yp) at increasing MOIs. LTB_4 was measured from supernatants 1 h post infection by ELISA. Each symbol represents an independent biological infection and the box plot represents the median of the group \pm the range. UI or 0 = uninfected. One-way ANOVA with Dunnett's *post hoc* test compared to uninfected. * = $p \leq 0.05$, ** = $p \leq 0.01$, # = $p \leq 0.0001$.

<https://doi.org/10.1371/journal.ppat.1011280.g004>

***Y. pestis* actively inhibits LTB₄ synthesis**

Seven Yop effectors are secreted via the T3SS [21–24], and Pulsifer et al. previously showed Yop effector-mediated inhibition of LTB₄ synthesis in human neutrophils by YpkA, YopE, YopJ, YopH, and YopT at an MOI of 100 [26]. However, Yop inhibition of LTB₄ synthesis by murine neutrophils has not been previously investigated, nor whether the same Yop effectors are sufficient to inhibit LTB₄ synthesis at a lower MOI. Therefore, murine and human neutrophils were infected at an MOI of 20 with a *Y. pestis* mutant strain that expresses the T3SS but lacks all seven Yop effectors (*Y. pestis* T3E) [50]. In contrast to *Y. pestis* infected cells, we observed a significant increase in LTB₄ synthesis in response to the *Y. pestis* T3E strain, indicating that the Yop effectors inhibit synthesis (Fig 5A and 5B; $p \leq 0.0001$). Moreover, when neutrophils were simultaneously infected with *Y. pestis* and the *Y. pestis* T3E mutant or *Y. pestis* and the *K. pneumoniae manC* mutant, LTB₄ levels were significantly lower than *Y. pestis* T3E or *K. pneumoniae manC* only infections (Fig 5C–5F; $p \leq 0.0001$). To determine if individual Yop effectors were sufficient to inhibit synthesis, murine neutrophils were infected with *Y. pestis* strains that expressed only one Yop effector [50]. LTB₄ synthesis was significantly decreased if *Y. pestis* expressed YpkA, YopE, YopH, or YopJ, and an intermediate phenotype was observed during infection with a strain expressing YopT (Fig 5G). These phenotypes recapitulated those previously reported for human neutrophils [26]. Together these data confirm that *Y. pestis* is not simply evading immune recognition but is actively inhibiting LTB₄ synthesis via the activity of multiple Yop effectors.

Neutrophils synthesize LTB₄ in response to the *Y. pestis* T3SS in the absence of the Yop effectors

Components of the T3SS are pathogen-associated molecular patterns (PAMPs) that are recognized by innate immune cells [7,51,52], suggesting that T3SS interactions with neutrophils may be responsible for the synthesis of LTB₄ during infections with the *Y. pestis* T3E strain. To test this hypothesis, we infected murine and human neutrophils with a *Y. pestis* strain lacking the pCD1 plasmid encoding the entire Ysc T3SS [*Y. pestis* T3⁽⁻⁾]. Unlike infections with *Y. pestis* T3E, we did not observe an increase in LTB₄ synthesis by neutrophils during interactions with *Y. pestis* T3⁽⁻⁾ compared to uninfected or *Y. pestis* infected cells, even after 2 h of infection (Fig 5A and 5B). Importantly, *Y. pestis* T3⁽⁻⁾ infection did not appear to result in increased neutrophil cell permeability or cytotoxicity (S2 Fig). To independently test that the T3SS is required to induce LTB₄ synthesis, *Y. pestis* T3E was cultured under conditions that alter the expression of the T3SS prior to infection of neutrophils [5,8,16]. Measuring expression of the LcrV protein as a proxy for overall T3SS expression confirmed decreased T3SS expression in cultures grown at 26°C compared to 37°C (Figs 6A and S3A). As predicted by the *Y. pestis* T3⁽⁻⁾ data, LTB₄ synthesis was not observed from neutrophils infected with *Y. pestis* T3E strains grown at 26°C, while synthesis was induced from bacteria cultured at 37°C (Fig 6B). No difference in bacterial viability between any of the *Y. pestis* strains was observed during the time frame of the experiment, diminishing the possibility that differences in neutrophil killing of the bacteria was responsible for these phenotypes (S3B Fig). Finally, neutrophils were infected with a *Y. pestis* T3E *yopB* mutant, which retains the other pCD1 encoded genes, but is defective in expression of the translocase that directly interacts with the host cell and is required for injection of the effector proteins [8,53–56]. Similar to the *Y. pestis* T3⁽⁻⁾ strain, the *Y. pestis* T3E *yopB* mutant did not induce LTB₄ synthesis, but synthesis was restored by *yopB* complementation (*yopB::cyopB*) (Fig 6C). Together, these data indicate that neutrophils recognize components of the *Y. pestis* T3SS as PAMPs, leading to the induction of LTB₄ synthesis, but only in the absence of the Yop effectors.

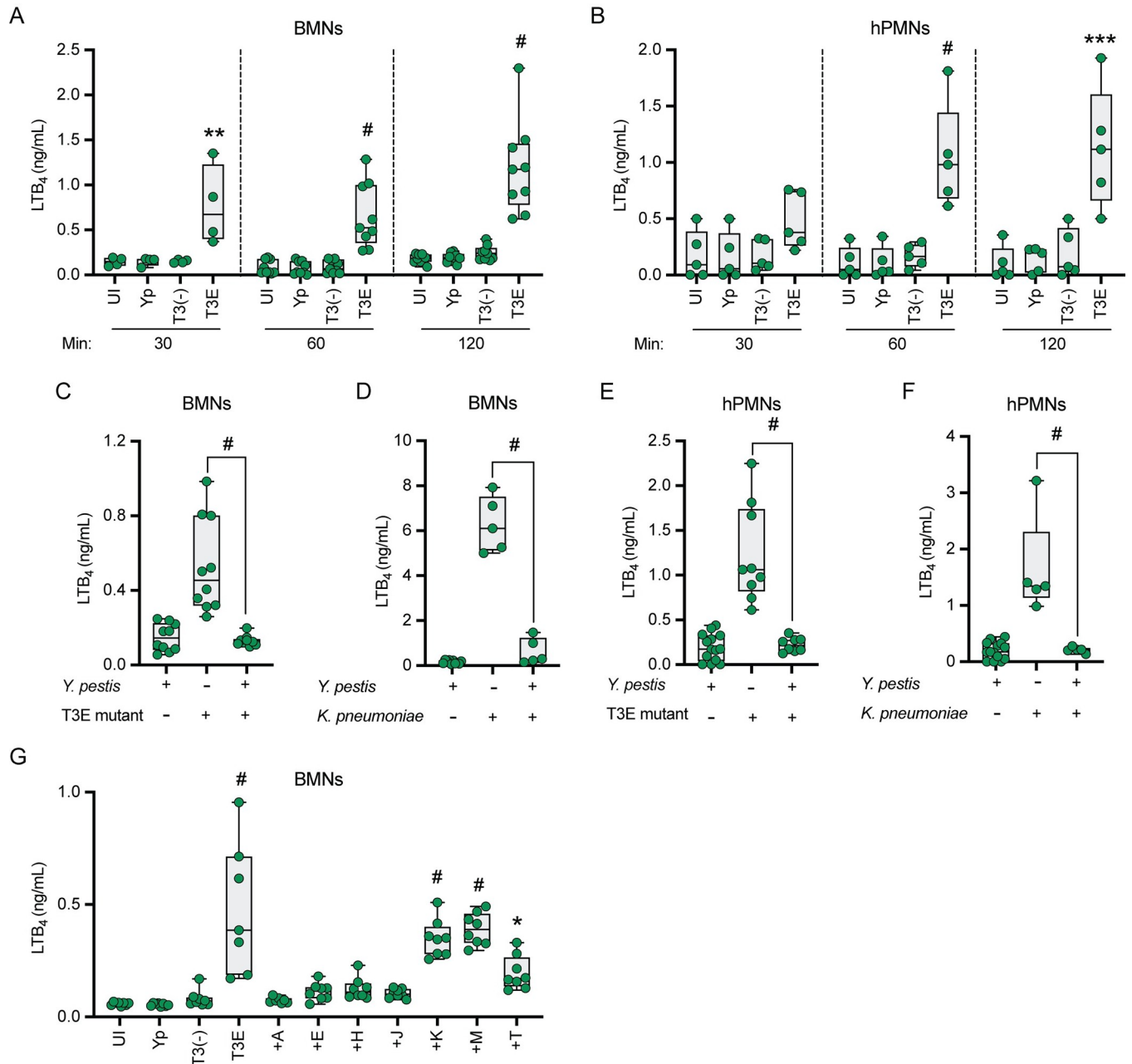


Fig 5. *Y. pestis* actively inhibits LTB₄ synthesis. (A) Murine (BMNs) or (B) human (hPMNs) neutrophils were infected with *Y. pestis* (Yp) or mutants that either lacked the Yop effectors (T3E) or the Yop effectors and the T3SS [T3(-)] at an MOI of 20 and LTB₄ was measured at 30, 60, or 120 min. (C and D) Murine (BMNs) or (E and F) human (hPMNs) neutrophils were co-infected with the indicated bacteria at a combined MOI of 20 and LTB₄ was measured at 60 min post-infection. (G) Murine neutrophils (BMNs) were infected with Yp, T3E, T3(-), or *Y. pestis* strains expressing only one Yop effector (+A = YpkA; +E = YopE; +H = YopH; +J = YopJ; +K = YopK; +M = YopM; or +T = YopT) at an MOI of 20 and LTB₄ was measured at 60 min post-infection. Each symbol represents an independent biological infection and the box plot represents the median of the group ± the range. UI = uninfected. One-way ANOVA with Dunnett's *post hoc* test compared to uninfected for A, B, and G, or Tukey's *post hoc* test compared to each condition for C, D, E, and F. * = $p \leq 0.05$, ** = $p \leq 0.01$, *** = $p \leq 0.001$, # = $p \leq 0.0001$.

<https://doi.org/10.1371/journal.ppat.1011280.g005>

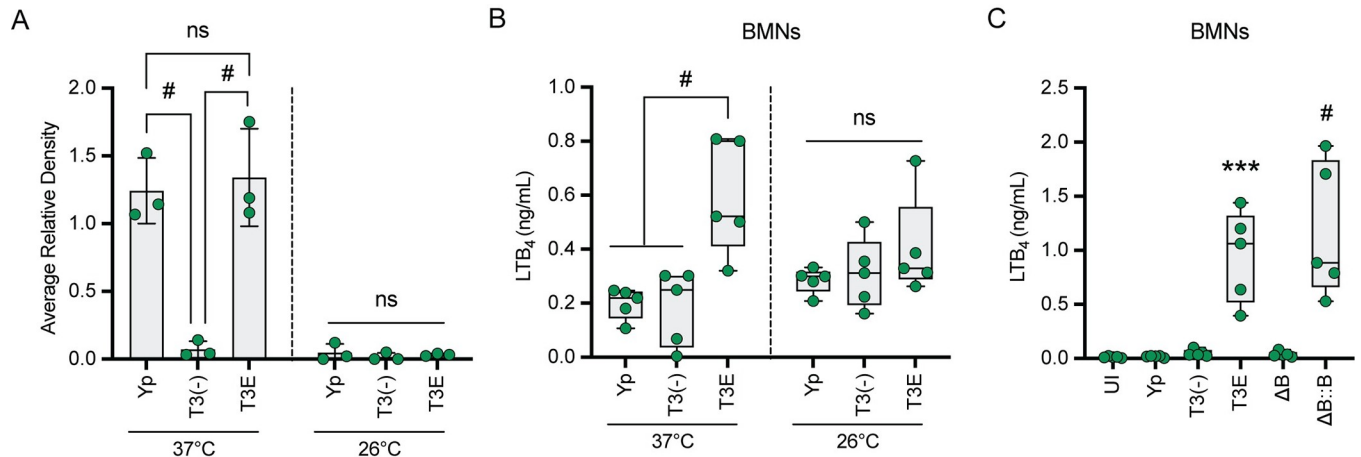


Fig 6. Neutrophils synthesize LTB₄ in response to the *Y. pestis* T3SS in the absence of the Yop effectors. (A) Relative expression of LcrV based on western blots normalized to total protein loaded from bacteria cultured at 37 or 26°C. (B) Murine neutrophils (BMNs) were infected (MOI of 20) with *Y. pestis* (Yp) or mutants that either lacked the Yop effectors (T3E) or the Yop effectors and the T3SS [T3(-)] cultured at 37 or 26°C and LTB₄ was measured at 60 min post-infection. (C) Murine neutrophils (BMNs) were infected (MOI of 20) with Yp, T3E, T3(-), a *yopB* mutant in the T3E background (ΔB), or ΔB complemented with *yopB* ($\Delta B::B$) cultured at 37°C and LTB₄ was measured at 60 min post-infection. Each symbol represents an independent biological infection and the box plot represents the median of the group \pm the range. One-way ANOVA with Tukey's *post hoc* test compared to each condition for A and B and Dunnett's *post hoc* test compared to uninfected for C. ns = not significant, *** = $p \leq 0.001$, # = $p \leq 0.0001$.

<https://doi.org/10.1371/journal.ppat.1011280.g006>

Y. pestis inhibition of LTB₄ synthesis is conserved during interactions with other leukocytes

In addition to neutrophils, two other lung resident leukocytes that can produce LTB₄ are mast cells and macrophages [33]. To determine if *Y. pestis* inhibits LTB₄ synthesis by these two cell types, bone marrow-derived mast cells and macrophages were isolated from C57BL/6J mice and infected with *Y. pestis*, *Y. pestis* T3E, or *Y. pestis* T3⁽⁻⁾. We observed no synthesis of LTB₄ by mast cells, even after 2 h of interacting with *Y. pestis* (Fig 7A). However, LTB₄ synthesis was significantly elevated in the absence of the Yop effectors (Fig 7A; $p \leq 0.01$), reaching levels

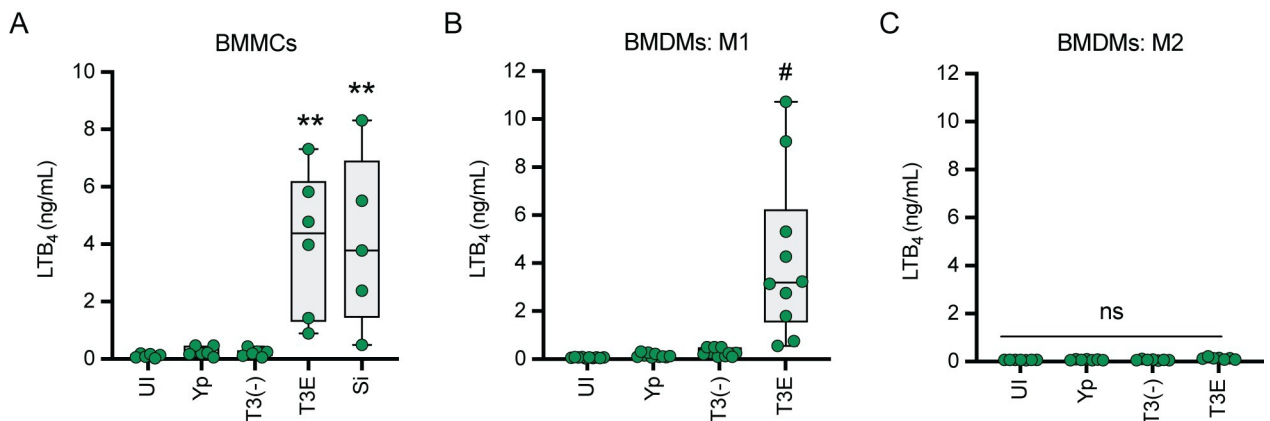


Fig 7. Lack of LTB₄ response to *Y. pestis* is conserved in other leukocytes. (A) Murine bone-marrow derived mast cells (BMMCs) were infected with *Y. pestis* (Yp) or with mutants that either lacked the Yop effectors (T3E) or the Yop effectors and the T3SS [T3(-)] at an MOI of 20, or treated with 100 mg/cm² crystalline silica (Si) and LTB₄ was measured at 2 h post-infection. (B and C) Murine bone-marrow derived macrophages (BMDMs) differentiated towards (B) M1 or (C) M2 phenotypes were infected with Yp, T3E, or T3(-) at an MOI of 20 and LTB₄ was measured at 4 h post-infection. UI = uninfected. Each symbol represents an independent biological infection and the box plot represents the median of the group \pm the range. One-way ANOVA with Dunnett's *post hoc* test compared to uninfected. ** = $p \leq 0.01$, # = $p \leq 0.0001$, ns = not significant.

<https://doi.org/10.1371/journal.ppat.1011280.g007>

similar to that of mast cells stimulated with crystalline silica, a potent inducer of LTB₄ synthesis [57,58]. LTB₄ synthesis by mast cells was also dependent on the presence of the T3SS, as the *Y. pestis* T3⁽⁻⁾ strain did not induce LTB₄ synthesis (Fig 7A). For macrophages, previous reports indicate that polarization influences the ability to produce LTB₄, with M1-polarized macrophages better able to synthesize LTB₄ in response to bacterial ligands than M2-polarized cells [59]. Therefore, we measured LTB₄ synthesis of both M1- and M2-polarized macrophages (S4 Fig). Again, we observed no significant synthesis of LTB₄ by either macrophage population during interactions with *Y. pestis*, even after 4 h post-infection (Fig 7B and 7C). However, significant synthesis of LTB₄ was observed in M1-polarized macrophages in response to the *Y. pestis* T3E strain, which was dependent on the presence of the T3SS (Fig 7B; $p \leq 0.0001$). As suggested by previous reports [60], we did not observe significant changes in LTB₄ synthesis by M2-polarized macrophages during interactions with any of the *Y. pestis* strains tested (Fig 7C). Together, these data indicate that mast cells and M1-polarized macrophages can synthesize LTB₄ in response to the *Y. pestis* T3SS, but the activity of the Yop effectors inhibits this response.

Discussion

A hallmark manifestation of plague is the absence of inflammation during the early stages of infection, which is critical to *Y. pestis* virulence [10,17,28,52]. While *Y. pestis* has been shown to actively dampen the host immune response, there is a gap in our understanding of the role of lipid mediators of inflammation during plague. This study sought to better define the host inflammatory lipid mediator response during pneumonic plague and expands our current understanding of how *Y. pestis* manipulates the immune system. During the earliest stages of infection, the host appears unable to initiate a timely LTB₄ response (Fig 1). Moreover, we demonstrated that exogenous treatment with LTB₄ can alter the host response to *Y. pestis* (Fig 3), suggesting that LTB₄ manipulation by *Y. pestis* contributes to disease outcome. Because LTB₄ is a potent chemoattractant crucial for rapid inflammation [31,32,61], a delay in LTB₄ synthesis during plague likely has a significant impact on the ability of the host to mount a robust inflammatory response needed to inhibit *Y. pestis* colonization. First, in the absence of LTB₄, sentinel leukocytes will not undergo autocrine signaling via LTB₄-BLT1. Because LTB₄-BLT1 engagement activates antimicrobial programs in leukocytes [31,32,46,62–64], the absence of autocrine signaling diminishes the ability of sentinel leukocytes directly interacting with *Y. pestis* to mount an effective antimicrobial response to kill the bacteria. LTB₄ synthesis is also regulated by BLT1 signaling, and autocrine signaling is required to amplify the production of LTB₄ needed to rapidly recruit additional tissue-resident immune cells to the site of infection [31,32,63,65,66]. Therefore, the normal feed-forward amplification of LTB₄ synthesis, which is key for a rapid response to a bacterial infection, will also be inhibited by *Y. pestis*. Second, because LTB₄ is required for neutrophil swarming [65,67,68], *Y. pestis* will also inhibit this key inflammatory mechanism [69]. Neutrophil swarming is required to contain bacteria at initial sites of infection [70,71]. Thus, while individual neutrophils may migrate towards sites of *Y. pestis* infection, effective neutrophil swarming of large populations of neutrophils will be diminished. Finally, LTB₄ is a diffusible molecule that can induce the inflammatory cascade in bystander cells [32,72]. Thus, while *Y. pestis* can inhibit cytokine and chemokine expression by cells with which it directly interacts [11,15], inhibition of LTB₄ synthesis likely also delays subsequent release of molecules by cells that do not directly interact with the bacteria. Together with the bacteria's other immune evasion mechanisms, inhibition of LTB₄ synthesis is likely another significant contributor to the generation of the non-inflammatory environment associated with the early stages of pneumonic plague [10,11,15]. Incorporating these new LTB₄

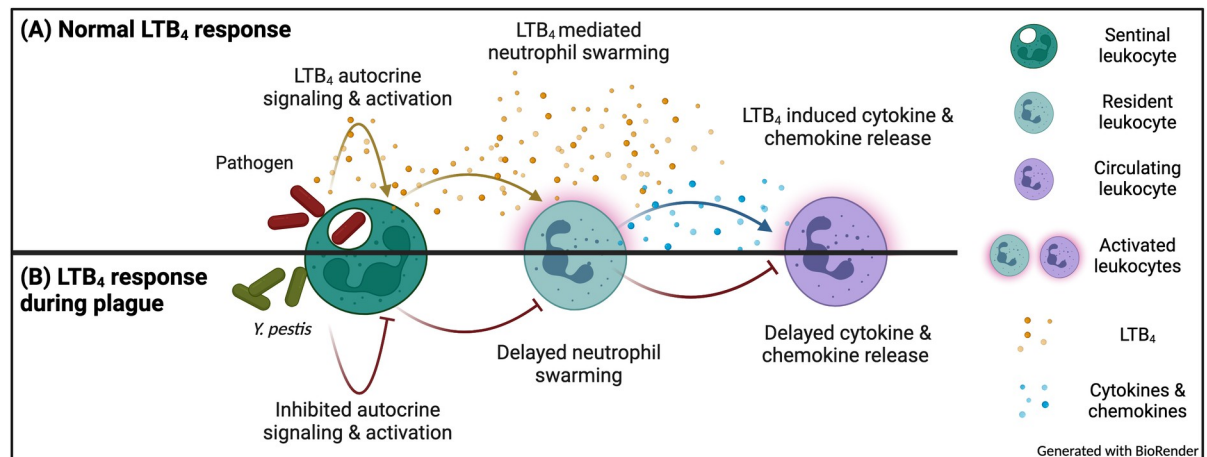


Fig 8. Working model for inhibition of the inflammatory cascade during plague. (A) Normal response by sentinel leukocytes results in rapid production of LTB₄ that leads to autocrine signaling, neutrophil swarming, and induction of cytokine and chemokine release. (B) *Y. pestis* inhibits the production of LTB₄ via the action of the Yop effectors, which delays resident neutrophil recruitment and subsequent production of cytokines and chemokines needed for inflammation.

<https://doi.org/10.1371/journal.ppat.1011280.g008>

data with published findings from other laboratories [10,11,15], we have updated our working model of *Y. pestis* inhibition of inflammation during pneumonic plague (Fig 8).

These studies also revealed that components of the T3SS trigger LTB₄ synthesis by leukocytes. Because our previous work with human samples indicated that neutrophils synthesize LTB₄ in response to *Y. pestis* in the absence of the T3SS [26], we were initially surprised that we did not observe LTB₄ synthesis by murine neutrophils to the *Y. pestis* T3⁽⁻⁾ strain. However, when we infected human neutrophils with lower MOIs, we observed that they also did not synthesize LTB₄ in the absence of the T3SS (Fig 5B). Under these infection conditions, neutrophils from both species only produced LTB₄ in response to *Y. pestis* expressing the T3SS but none of the Yop effectors. These data support that components of the T3SS are PAMPs produced by *Y. pestis* that are not only recognized by macrophages [73] but also by neutrophils. While previous studies have indicated that the Yop effectors are PAMPs in neutrophils [74,75], to our knowledge the data presented here represent the first example that non-effector components of the *Y. pestis* T3SS can also be recognized as a PAMP by neutrophils. In macrophages, in the absence of the Yop effectors, interactions with the T3SS, notably the translocon proteins YopB and YopD, induce NLRP3-dependent activation of the caspase 1 inflammasome, IL1-β secretion, and pyroptosis [54,76], suggesting that inflammasome activation may contribute to LTB₄ synthesis during interactions with *Y. pestis* T3E. However, whether inflammasome activation is required for the *Y. pestis* T3SS-mediated LTB₄ synthesis remains unclear, as LTB₄ synthesis in response to other stimuli is not dependent on inflammasome activation [57,77,78]. Interestingly, infection of neutrophils with a strain of *Y. pestis* that only expresses YopK, which has been reported to inhibit NLRP3 inflammasome activation in macrophages [53,54], does not inhibit LTB₄ synthesis (Fig 4C) [26], supporting the possibility that LTB₄ synthesis may not be dependent on inflammasome activation in neutrophils. Future studies using neutrophils from mice defective in specific NLRs and caspases will allow us to definitively determine if inflammasome activation is required for LTB₄ synthesis in response to the *Y. pestis* T3SS. We have also confirmed that four Yop effectors, YpkA, YopE, YopJ, and YopH are sufficient to inhibit LTB₄ synthesis by both human and murine neutrophils. Synthesis of LTB₄ requires MAPK- and Ca²⁺-dependent activation of cPLA2 and 5-LOX [34,79]. Previous work, primarily in macrophages, has shown that both of these signaling pathways are efficiently inhibited by these

four Yop effectors [8,20,80–84], suggesting that subversion of MAPK and Ca²⁺ signaling by *Y. pestis* is responsible for inhibition of LTB₄ synthesis. Supporting this hypothesis, Pulsifer et al. demonstrated that inhibition of ERK phosphorylation by YopJ is sufficient to inhibit LTB₄ synthesis by human neutrophils [26]. Defining the specific molecular mechanisms employed by YpkA, YopE, and YopH to inhibit LTB₄ synthesis will be important in better understanding *Y. pestis* virulence and is a long-term goal.

One of the key antimicrobial mechanisms inhibited by the Yop effectors is phagocytosis [5,16,85,86], and Hedge et al. have previously shown that phagocytosis of crystalline silica is required for LTB₄ synthesis in that model of sterile inflammation [57]. These data raise the possibility that inhibition of phagocytosis by *Y. pestis* may not only inhibit bacterial killing, but LTB₄ synthesis and rapid initiation of inflammatory programming in neutrophils. Studies to delineate the contribution of phagocytosis to LTB₄ synthesis are ongoing, but the differences in LTB₄ synthesis by cells infected with *Y. pestis* T3E and *Y. pestis* T3⁽⁻⁾ suggest that phagocytosis alone is not sufficient to trigger LTB₄ synthesis in the absence of proper PAMPs, in this case components of the T3SS. Moreover, the lack of LTB₄ synthesis in response to *Y. pestis* T3⁽⁻⁾ also differed from what we observed for other gram-negative bacteria without a T3SS (*E. coli* and *K. pneumoniae*), indicating that *Y. pestis* may also mask other potential gram-negative PAMPs that would typically be recognized by neutrophils. These data support that *Y. pestis* has evolved both active (via the Yop effectors) and passive mechanisms to evade immune recognition and induction of LTB₄ synthesis. It is worth noting that unlike human neutrophils, murine neutrophils did not appear to synthesize LTB₄ during infections with the T3⁽⁻⁾ strain at high MOIs (S5 Fig). Differences in neutrophil responses between the two species have been well documented [87–91], but these observations merit further investigation into LTB₄ responses by human neutrophils using higher MOIs to determine if human neutrophils are able to recognize other PAMPs during *Y. pestis* infection.

Finally, while we focused primarily on LTB₄ in this study, we also observed changes in the synthesis of other lipids during plague that merit future considerations (S1 Table). The rapid cyclooxygenase response raises questions about whether prostaglandins are protective or detrimental during pneumonic plague. Historically, prostaglandins were thought to promote inflammation, but these mediators appear more nuanced under closer scrutiny and can just as likely inhibit inflammation, as well as participate in normal development physiology, without eliciting inflammation [42,43,92]. The prostaglandins we observed as being significantly elevated during the non-inflammatory stage of pneumonic plague—PGA₂, PGD₂, PGE₂, and PGJ₂—have been shown to inhibit inflammation in various models, especially as concentrations increase [42,43,93–95]. PGE₂ can inhibit NADPH oxidase activity during infection with *K. pneumoniae*, which suppressed bacterial killing [96], and directly counteracts the proinflammatory activities of LTB₄ [97,98]. The phagocytic index of LTB₄-stimulated rat alveolar macrophages (AMs) is reduced when co-stimulated with PGE₂ [98]. Moreover, AMs treated with PGE₂ showed a 40% reduction in LTB₄ synthesis when stimulated with an ionophore known to induce a strong LTB₄ response [97]. This inhibition of LTB₄ by PGE₂ is suspected to be via an increase in second messenger cAMP that activates protein kinase A (PKA), which has been shown to inhibit LTB₄ synthesis [97,99]. Together, these data suggest that the elevated levels of prostaglandin synthesis observed during pneumonic plague may contribute to the blunted LTB₄ response by the host.

In conclusion, we have defined the kinetics of the key inflammatory lipid mediator LTB₄ during pneumonic plague, which revealed a blunted response during the early stages of infection. Furthermore, we have shown that *Y. pestis* actively manipulates LTB₄ synthesis by leukocytes via the activity of Yop effectors to generate a beneficial inflammatory outcome to the pathogen. These discoveries warrant further research into the role of lipids, and subsequent

manipulation of their synthesis by *Y. pestis*, to fully understand the molecular mechanisms *Y. pestis* has evolved to manipulate the mammalian immune response.

Material and methods

Ethics statement

All animal work was approved by the University of Louisville Institutional Animal Care and Use Committee (IACUC Protocol #22157). Use of human neutrophils was approved by the University of Louisville Institutional Review Board guidelines (IRB #96.0191) and written consents for use were obtained.

Bacterial strains

Bacterial strains used in this study are listed in [S2 Table](#). For mouse infections, *Y. pestis* was grown at 26°C for 6–8 h, diluted to an optical density (OD) (600 nm) of 0.05 in Bacto brain heart infusion (BHI) broth (BD Biosciences Cat. No. 237500) with 2.5 mM CaCl₂ and then grown at 37°C with aeration for 15–18 h [100]. For cell culture infections, *Y. pestis* was cultured with BHI broth for 15–18 h at 26°C in aeration. Cultures were then diluted 1:10 in fresh, warmed BHI broth containing 20 mM MgCl₂ and 20 mM Na-oxalate and cultured at 37°C for 3 h with aeration to induce expression of the T3SS. Bacterial concentrations were determined using a spectrophotometer and diluted to desired concentrations in 1 × Dulbecco's phosphate-buffered saline (DPBS) for mouse infections or fresh medium for *in vitro* studies. Concentrations of bacterial inoculums for mouse studies were confirmed by serial dilution and enumeration on BHI agar plates.

Mouse infections

All animal work was performed at least twice to ensure reproducibility. 6–8 week-old C57BL/6J or BLT1^{-/-} [49] male and female mice were infected with *Y. pestis* KIM5+ or *Y. pestis* CO92 LUX_{pcysZK}. For lipid measurements, mice were anesthetized with ketamine/xylazine and administered 20 μL of *Y. pestis* KIM5+ suspended in 1 × DPBS to the left nare as previously described [48,100]. Mice were monitored for the development of moribund disease symptoms twice daily and humanely euthanized when they met previously approved end point criteria. At 6, 12, 24, 36, or 48 h, mice were humanely euthanized by CO₂ asphyxiation and lungs were harvested and lung masses recorded. Lungs were transferred to a 2 mL tube pre-filled with 2.8 mm ceramic beads (VWR, Cat. No. 10158–612), flash frozen on dry ice, and stored at -80°C until preparation for lipid analysis. For CFU studies, mice were humanely euthanized by CO₂ asphyxiation at 12 or 24 h and lungs were harvested. Lungs were transferred to Whirl Pak's containing 1 mL of 1 × DPBS, and gently homogenized using a serological pipette. Homogenized tissues were serially diluted and plated onto BHI agar. After 2 days of incubation at 26°C, bacteria were enumerated. For optical imaging and survival curves, mice were infected with *Y. pestis* CO92 LUX_{pcysZK} and monitored for bacterial proliferation as a function of bioluminescence by optical imaging and for the development of moribund disease. At each time point, mice were anesthetized with isoflurane and imaged using the IVIS Spectrum imaging system (Caliper Life Sciences, Hopkinton, MA). Average radiance (photons/s/cm²) was calculated for the lungs as previously described [48]. For the exogenous LTB₄ treatment, mice were intraperitoneally injected with 1 × DPBS or 10 nmol LTB₄ (Cayman Chemical Cat. No. 20110). At 1 h post-treatment, mice were administered 10⁵ CFU of *Y. pestis* KIM5+ via intraperitoneal injection. At 3 h post infection, mice were humanely euthanized, and the peritoneal cavity was

washed and collected using 2 lavages of 1 mL of 1 x DPBS. Lavages were used for CFU enumeration or neutrophil quantification by flow cytometry.

Lipid extraction and quantification by LC-MS

To quantify LTB₄ abundance from whole lungs, lungs were thawed with 1.8 mL of ice cold 75% methanol + 0.1% BHT for 3 minutes. Lungs were then homogenized with a Bead Ruptor 4 (OMNI) at speed 5 (5 m/s) for 4 cycles of 45 seconds with 1-minute pauses in which the lungs were placed on ice. Tissue debris was then centrifuged for 10 min at 1,500 x g at 4°C. The supernatant (~1.5 mL) was then transferred to a fresh eppendorf tube, incubated at 4°C for 24 h to inactivate *Y. pestis* and extract lipids. After successful inactivation, samples were removed from BSL3 containment and stored at -80°C. Lipid extraction was then performed as previously described [101]. For the expanded global lipid analysis, lungs were thawed with 1.5 mL of ice cold 1 x DPBS + HALT protease and phosphatase inhibitor cocktail for 3 minutes. Lungs were then homogenized with a Bead Ruptor 4. Tissue debris was then centrifuged for 10 min at 1,500 x g at 4°C. The supernatant (~1.5 mL) was then transferred to a fresh eppendorf tube. From this, 250 µL of supernatant was combined with 750 µL of 100% methanol + 0.1% BHT (final concentration of 75%) and incubated at 4°C for 24 h to inactivate *Y. pestis* and extract lipids. After confirmation of successful inactivation of *Y. pestis*, lipids were extracted and quantified by the Wayne State University Lipidomics Facility as previously described [102]. The extracted samples were analyzed for the fatty acyl lipidome using standardized methods as described previously [103,104].

Flow cytometry

To quantify the neutrophil population from peritoneal lavages, cells were labeled with anti-Ly6G antibody (1:400; BD Pharmingen Cat. No. 551460) and anti-CD11b antibody (1:600; Biolegend Cat. No. 101212) for 1 h on ice, in the dark. Cells were pelleted and resuspended in 1% PFA. Single cell suspensions were generated by straining with 70 µM mesh prior to analysis on the flow cytometer. Neutrophils were identified as cells with high expression of Ly6G and CD11b and data is represented as the percent of the population that were classified as neutrophils. An example of the gating strategy is shown in [S1 Fig](#).

Cell isolation and cultivation

Human neutrophils were isolated from the peripheral blood of healthy, medication-free donors, as described previously [105]. Briefly, white blood cells were isolated from whole blood using a 6% dextran solution. Neutrophils were then separated from monocytes using a percoll gradient of 42% and 50.5%. RBCs were then lysed from the neutrophil containing layer using 0.2% NaCl for 30 seconds and followed by a quench with 5 mL 1.6% NaCl. Neutrophil isolations yielded ≥ 95% purity and were used within 1 h of isolation. Murine neutrophils were isolated from bone marrow of 7-12-week-old mice using an Anti-Ly-6G Microbeads kit (Miltenyi Biotec Cat. No. 130-120-337) per the manufacturer's instructions. Neutrophil isolations yielded ≥ 95% purity and were used within 1 h of isolation. Macrophages were differentiated from murine bone marrow in DMEM supplemented with 1 mM Na-pyruvate and 10% FBS for 6 days. Macrophages were either polarized with 10 ng/mL of GM-CSF (M1; Kingfisher Biotech Cat. No. RP0407M) or with 30% L929 conditioned media and 10 ng/mL of M-CSF (M2; Kingfisher Biotech Cat. No. RP0462M) throughout the differentiation. The medium was replaced on days 1 and 3 (adapted from [106]). Polarization was confirmed by qRT-PCR, as previously described [107], using markers for M1 and M2 phenotypes, TNF-α and Il-10, respectively ([S4 Fig](#)). Murine mast cells were isolated and differentiated from bone marrow as

previously described [108]. Briefly, isolated bone marrow cells were resuspended in BMMC culture medium [DMEM containing 10% FCS, penicillin (100 units/mL), streptomycin (100 mg/mL), 2 mmol/L L-glutamine, and 50 mmol/L β -mercaptoethanol] supplemented with recombinant mouse stem cell factor (SCF) (12.5 ng/mL; R&D Systems Cat. No. 455-MC) and recombinant mouse IL-3 (10 ng/mL; R&D Systems Cat. No. 403-ML). Cells were plated at a density of 1×10^6 cells/mL in a T-75 cm² flask. Nonadherent cells were transferred after 48 hours into fresh flasks without disturbing the adherent (fibroblast) cells. Mast cells were visible after 4 weeks of culture and propagated further or plated for experiments in DMEM without antibiotics.

Leukocyte infections

Human neutrophils were resuspended in Kreb's buffer (w/ Ca²⁺ and Mg²⁺) then adhered to 24-well plates for 30 min that were coated with pooled human serum prior to infection (wells were washed twice with 1 x DPBS prior to plating the cells). Murine bone marrow neutrophils were resuspended in RPMI + 5% FBS then adhered to 24-well plates for 30 min that were coated with FBS prior to infection (wells were washed twice with 1 x DPBS prior to plating the cells). Neutrophils were infected at a multiplicity of infection (MOI) of 20, 50, or 100 and incubated for 1 h in a cell culture incubator at 37°C with a constant rate of 5% CO₂. Co-infections were performed at a final MOI of 20 (MOI of 10 for each strain). 1 h post-infection, supernatants were collected, centrifuged for 1 min at 6,000 x g, and supernatants devoid of cells were transferred to a fresh eppendorf tube. Macrophages were adhered to 24-well plates in DMEM + 10% FBS 1 day prior to infection. Macrophages were infected at an MOI of 20. At 4 h post-infection, supernatants were collected, centrifuged for 1 min at 6,000 x g, and supernatants devoid of cells were transferred to a fresh eppendorf tube. Mast cells were adhered to 24-well plates in DMEM only for 1 h prior to infection. Mast cells were infected at an MOI of 20 or treated with crystalline silica (100 mg/cm²). At 2 h post-infection supernatants were collected, centrifuged for 1 min at 6,000 x g, and supernatants devoid of cells were transferred to a fresh eppendorf tube. All infections were synchronized by centrifugation (200 x g for 5 min). All samples were stored at -80°C until ELISA.

Measurement of LTB₄ by enzyme-linked immunosorbent assay

Supernatants of neutrophils, macrophages, and mast cells were collected and measured for LTB₄ by ELISA per manufacturer's instructions (Cayman Chemicals Cat. No. 520111).

Cell viability assays

To determine leukocyte permeability, cells were incubated with trypan blue for 5 min and trypan blue exclusion was measured using SD100 counting chambers (VWR Cat. No. MSPP-CHT4SD100) and a cell counter (Nexcelom Cellometer Auto T4). To determine leukocyte cytotoxicity, lactate dehydrogenase (LDH) was measured from leukocyte supernatants using the CytoTox 96 Non-Radioactive Cytotoxicity kit (Promega Cat. No. g1780) per the manufacturer's instructions.

Bacterial viability assays

To measure bacterial viability during interactions with neutrophils, murine neutrophils were resuspended in RPMI + 5% FBS then adhered to 96-well white bottom plates for 30 min coated with FBS prior to infection (wells were washed twice with 1 x DPBS prior to plating the cells). Neutrophils were infected at an MOI of 20, centrifuged for 5 min at 200 x g, and bacterial

viability was measured as a function of bioluminescence using a plate reader (BioTek Cytation 1 imaging reader).

Measurement of LcrV by western blot

Bacterial strains were cultured with BHI broth for 15–18 h at 26°C in aeration. Cultures were then diluted 1:10 in fresh warmed BHI broth containing 20 mM MgCl₂ and 20 mM Na-oxalate and cultured at 37 or 26°C for 3 h. 1 OD₆₀₀ of bacterial pellets were collected and resuspended in 1 x SDS-PAGE loading buffer, boiled for 10 min, and 0.1 OD₆₀₀ was separated on a 10% SDS-PAGE gel. As a positive control, 0.2 g of recombinant LcrV protein was used (BEI resources Cat. No. NR-32875). Samples were immunoblotted with polyclonal anti-LcrV antibody diluted to 1:4,000 (BEI Resources Cat. No. NR-31022). Anti-goat IgG HRP secondary antibody was diluted to 1:5,000 (Bio-Techne Cat. No. HAF017). Densitometry was performed using ImageJ software to compare LcrV bands between samples [109].

Statistics

For all studies, male and female mice or human donors were used and no sex biases were observed for any phenotype. All *in vivo* experiments were repeated at least twice and *in vitro* experiments at least 5 times. Where noted in the figure legends, figures may represent the combined data from multiple biologically independent experiments. For *in vitro* experiments, each data point represents data from biologically independent experiments performed on different days. Where appropriate and as indicated in the figure legends, statistical comparisons were performed with Prism (GraphPad) using one-way analysis of variance (ANOVA) with Dunnett's or Tukey's *post hoc* test, T-test with Mann-Whitney's *post hoc* test, or Log-Rank analysis. P values ≤ 0.05 were considered statistically significant and reported. For LC-MS analysis of lipids, a LIMMA—Moderated T-test was performed using a modified version of a previously published protocol using R packages [110–112]. Briefly, raw data were transformed by taking logarithmic base 2 followed by quantile normalization. Missing values were then ascribed using a singular value decomposition method. Lipids missing > 40% of the values were excluded from subsequent analysis. Finally, differentially abundant lipids (p ≤ 0.05) were further filtered by fold-change (FC) criteria (1 < log₂FC < 1) and multiple comparisons testing with a false discovery rate.

Supporting information

S1 Fig. Gating strategy for identifying neutrophil populations in the peritoneal cavity.

Example gating strategy from the PBS-treated group from Fig 3A.

(TIF)

S2 Fig. Absence of LTB₄ response to *Y. pestis* is not due to cell death. (A–D) Murine (BMNs) or (E–F) human (hPMNs) neutrophils were infected with *Y. pestis* (Yp) or mutants that either lacked the Yop effectors (T3E) or lacked the Yop effectors and the T3SS [T3(-)] at the indicated MOIs and cell permeability as a function of trypan exclusion or cytotoxicity as a function of LDH release was measured at 1 h post-infection. Each symbol represents an independent biological infection and the box plot represents the median of the group ± the range. UI = uninfected. One-way ANOVA with Dunnett's *post hoc* test compared to uninfected. * = p ≤ 0.05, ** = p ≤ 0.01, *** = p ≤ 0.001, # = p ≤ 0.0001.

(TIF)

S3 Fig. Expression of T3SS needle required for LTB₄ synthesis in response to *Y. pestis*.

(A) Representative western blot and Coomassie images of *Y. pestis* lysates (0.1 OD; 1 OD = 3 × 10⁸

CFU) harvested from cultures grown at 37°C or 26°C used for densitometry reported in Fig 6A. (B) Bacterial viability measured by a function of bioluminescence after 1 h infection of neutrophils. + or Yp = *Y. pestis*, — or T3(-) = *Y. pestis* T3(-); E or T3E = *Y. pestis* T3E; LcrV = 0.2 µg recombinant LcrV protein. Each symbol represents an independent biological infection and the bar graph represents the mean ± the standard deviation. One-way ANOVA with Tukey's *post hoc* test compared to each condition. ns = not significant. (TIF)

S4 Fig. M1 polarization required for macrophage synthesis towards *Y. pestis* T3SS.

qRT-PCR measurement of TNF-α and IL-10 in murine BMDMs differentiated towards M1 or M2. Each symbol represents an independent biological sample and the box plot represents the median of the group ± the range. T-test with Mann-Whitney's *post hoc* test. * = $p \leq 0.05$, ** = $p \leq 0.01$. (TIF)

S5 Fig. Differential recognition of T3⁽⁻⁾ *Y. pestis* between human and mice neutrophils. (A)

Murine (BMNs) or (B) human (hPMNs) neutrophils were infected with *Y. pestis* (Yp) or mutants that either lacked the Yop effectors (T3E) or lacked the Yop effectors and the T3SS [T3(-)] at the indicated MOIs and LTB₄ was measured 1 h post-infection. Each symbol represents an independent biological infection and the box plot represents the median of the group ± the range. UI = uninfected. One-way ANOVA with Dunnett's *post hoc* test compared to uninfected. *** = $p \leq 0.001$, # = $p \leq 0.0001$. (TIF)

S1 Table. Changes in inflammatory lipids during first 48h of pneumonic plague. C57BL/6J mice were infected with 10 x the LD₅₀ of *Y. pestis* KIM5+ and lungs were harvested at 6, 12, 24, 36, and 48 h post-infection (n = 5). Total lipids were isolated from homogenized lungs and lipids were quantified by LC-MS. Significant changes in lipid concentrations were observed in at least one time point for 63 lipids. Lipids that were below the limit of detection for all time points were excluded from statistical analysis.

(XLSX)

S2 Table. Bacterial strains and plasmids used in this study.

(DOCX)

Acknowledgments

The authors would like to acknowledge Dr. Jon Goguen for generously sharing the *Yersinia pestis* KIM1001 strains and Dr. Jonathan M. Warawa for generously sharing the *K. pneumoniae* Δ*amanC* strain. The following reagents were obtained through BEI Resources, NIAID, NIH: *Yersinia pestis* LcrV Protein, Recombinant from *Escherichia coli*, NR-32875, and Polyclonal Anti-*Yersinia pestis* V-Antigen (LcrV) (antiserum, Goat), NR-31022.

Author Contributions

Conceptualization: Amanda Brady, Bodduluri Haribabu, Silvia M. Uriarte, Matthew B. Lawrenz.

Formal analysis: Amanda Brady, Jianmin Pan, Nolan L. Boyd, Jing-Juan Zheng, Shesh N. Rai, Jason Hellmann, Matthew B. Lawrenz.

Funding acquisition: Amanda Brady, Krishna Rao Maddipati, Jason Hellmann, Matthew B. Lawrenz.

Investigation: Amanda Brady, Katelyn R. Sheneman, Amanda R. Pulsifer, Sarah L. Price, Taylor M. Garrison, Krishna Rao Maddipati, Sobha R. Bodduluri.

Methodology: Amanda Brady, Silvia M. Uriarte, Matthew B. Lawrenz.

Project administration: Matthew B. Lawrenz.

Resources: Krishna Rao Maddipati, Jason Hellmann, Bodduluri Haribabu, Silvia M. Uriarte, Matthew B. Lawrenz.

Supervision: Matthew B. Lawrenz.

Validation: Amanda Brady.

Visualization: Amanda Brady, Matthew B. Lawrenz.

Writing – original draft: Amanda Brady, Matthew B. Lawrenz.

Writing – review & editing: Amanda Brady, Krishna Rao Maddipati, Shesh N. Rai, Bodduluri Haribabu, Silvia M. Uriarte, Matthew B. Lawrenz.

References

1. Frith J. The history of plague—Part 1. The three great pandemics. *J Mil Vet Health*. 2012; 20(2):11–6. <https://doi.org/10.2021-22485863/JMVH>
2. Bertherat E. Plague around the world, 2010–2015. World Health Organization. 2016; 8(91):89–104.
3. Gage KL, Kosoy MY. Natural history of plague: Perspectives from more than a century of research. *Annu Rev Entomol*. 2005; 50:505–28. Epub 2004/10/09. <https://doi.org/10.1146/annurev.ento.50.071803.130337> PMID: 15471529.
4. Nelson CA, Meaney-Delman D, Fleck-Derderian S, Cooley KM, Yu PA, Mead PS. Antimicrobial treatment and prophylaxis of plague: recommendations for naturally acquired infections and bioterrorism response. *Morb Mortal Weekly Rep*. 2021; 70(3). <https://doi.org/10.15585/mmwr.rr7003a1> PMID: 34264565
5. Perry RD, Fetherston JD. *Yersinia pestis*—Etiologic agent of plague. *Clin Microbiol Rev*. 1997; 10(1):35–66. <https://doi.org/10.1128/cmr.10.1.35> PMID: 8993858
6. Eisen RJ, Dennis DT, Gage KL. The role of early-phase transmission in the spread of *Yersinia pestis*. *J Med Entomol*. 2015; 52(6):1183–92. Epub 2015/09/04. <https://doi.org/10.1093/jme/tjv128> PMID: 26336267; PubMed Central PMCID: PMC4636957.
7. Coburn B, Sekirov I, Finlay BB. Type III secretion systems and disease. *Clin Microbiol Rev*. 2007; 20(4):535–49. Epub 2007/10/16. <https://doi.org/10.1128/CMR.00013-07> PMID: 17934073; PubMed Central PMCID: PMC2176049.
8. Dewoody RS, Merritt PM, Marketon MM. Regulation of the *Yersinia* type III secretion system: traffic control. *Front Cell Infect Microbiol*. 2013; 3:4. Epub 2013/02/08. <https://doi.org/10.3389/fcimb.2013.00004> PMID: 23390616; PubMed Central PMCID: PMC3565153.
9. Straley SC, Skrzypek E, Plano GV, Bliska JB. Yops of *Yersinia* spp. pathogenic for humans. *Infect Immun*. 1993; 61(8). <https://doi.org/10.1128/iai.61.8.3105-3110.1993>
10. Bosio CF, Jarrett CO, Gardner D, Hinnebusch BJ. Kinetics of innate immune response to *Yersinia pestis* after intradermal infection in a mouse model. *Infect Immun*. 2012; 80(11):4034–45. Epub 2012/09/12. <https://doi.org/10.1128/IAI.00606-12> PMID: 22966041; PubMed Central PMCID: PMC3486050.
11. Lathem WW, Crosby SD, Miller VL, Goldman WE. Progression of primary pneumonic plague A mouse model of infection, pathology, and bacterial transcriptional activity. *PNAS*. 2005; 102(49):17786–91. <https://doi.org/10.1073/pnas.0506840102> PMID: 16306265
12. Banerjee SK, Crane SD, Pechous RD. A dual role for the plasminogen activator protease during the preinflammatory phase of primary pneumonic plague. *J Infect Dis*. 2020; 222(3):407–16. Epub 2020/03/05. <https://doi.org/10.1093/infdis/jiaa094> PMID: 32128567; PubMed Central PMCID: PMC7336565.
13. Cantwell AM, Bubeck SS, Dube PH. YopH inhibits early pro-inflammatory cytokine responses during plague pneumonia. *BMC Immunol*. 2010; 11(29). <https://doi.org/10.1186/1471-2172-11-29> PMID: 20565713

14. Peters KN, Dhariwala MO, Hughes Hanks JM, Brown CR, Anderson DM. Early apoptosis of macrophages modulated by injection of *Yersinia pestis* YopK promotes progression of primary pneumonic plague. *PLoS Pathog.* 2013; 9(4):e1003324. Epub 2013/05/02. <https://doi.org/10.1371/journal.ppat.1003324> PMID: 23633954; PubMed Central PMCID: PMC3636031.
15. Bubeck SS, Cantwell AM, Dube PH. Delayed inflammatory response to primary pneumonic plague occurs in both outbred and inbred mice. *Infect Immun.* 2007; 75(2):697–705. Epub 2006/11/15. <https://doi.org/10.1128/IAI.00403-06> PMID: 17101642; PubMed Central PMCID: PMC1828510.
16. Plano GV, Schesser K. The *Yersinia pestis* type III secretion system: expression, assembly and role in the evasion of host defenses. *Immunol Res.* 2013; 57(1–3):237–45. Epub 2013/11/08. <https://doi.org/10.1007/s12026-013-8454-3> PMID: 24198067.
17. Demeure C, Dussurget O, Fiol GM, Le Guern AS, Savin C, Pizarro-Cerda J. *Yersinia pestis* and plague: an updated view on evolution, virulence determinants, immune subversion, vaccination and diagnostics. *Microbes Infect.* 2019; 20(5):357–70. Epub 2019/06/30. <https://doi.org/10.1038/s41435-019-0065-0> PMID: 31252217.
18. Marketon MM, DePaolo RW, DeBord KL, Jabri B, Schneewind O. Plague bacteria target immune cells during infection. *Science.* 2005; 309(5741):1739–41. Epub 2005/07/30. <https://doi.org/10.1126/science.1114580> PMID: 16051750; PubMed Central PMCID: PMC3210820.
19. Pechous RD, Sivaraman V, Price PA, Stasulli NM, Goldman WE. Early host cell targets of *Yersinia pestis* during primary pneumonic plague. *PLoS Pathogens.* 2013; 9(10):e1003679. Epub 2013/10/08. <https://doi.org/10.1371/journal.ppat.1003679> PMID: 24098126; PubMed Central PMCID: PMC3789773.
20. Rolan HG, Durand EA, Mecas J. Identifying *Yersinia* YopH-targeted signal transduction pathways that impair neutrophil responses during *in vivo* murine infection. *Cell Host Microbe.* 2013; 14(3):306–17. Epub 2013/09/17. <https://doi.org/10.1016/j.chom.2013.08.013> PMID: 24034616; PubMed Central PMCID: PMC3789382.
21. Dudte SC, Hinnebusch BJ, Shannon JG. Characterization of *Yersinia pestis* interactions with human neutrophils *In vitro*. *Front Cell Infect Microbiol.* 2017; 7:358. Epub 2017/08/30. <https://doi.org/10.3389/fcimb.2017.00358> PMID: 28848716; PubMed Central PMCID: PMC5552669.
22. Spinner JL, Cundiff JA, Kobayashi SD. *Yersinia pestis* type III secretion system-dependent inhibition of human polymorphonuclear leukocyte function. *Infect Immun.* 2008; 76(8):3754–60. Epub 2008/05/21. <https://doi.org/10.1128/IAI.00385-08> PMID: 18490459; PubMed Central PMCID: PMC2493194.
23. Spinner JL, Hasenkrug AM, Shannon JG, Kobayashi SD, Hinnebusch BJ. Role of the *Yersinia* YopJ protein in suppressing interleukin-8 secretion by human polymorphonuclear leukocytes. *Microbes Infect.* 2016; 18(1):21–9. Epub 2015/09/13. <https://doi.org/10.1016/j.micinf.2015.08.015> PMID: 26361732; PubMed Central PMCID: PMC4715925.
24. Spinner JL, Seo KS, O'Loughlin JL, Cundiff JA, Minnich SA, Bohach GA, et al. Neutrophils are resistant to *Yersinia* YopJ/P-induced apoptosis and are protected from ROS-mediated cell death by the type III secretion system. *PLoS ONE.* 2010; 5(2):e9279. Epub 2010/02/23. <https://doi.org/10.1371/journal.pone.0009279> PMID: 20174624; PubMed Central PMCID: PMC2823771.
25. Eichelberger KR, Jones GS, Goldman WE. Inhibition of Neutrophil Primary Granule Release during *Yersinia pestis* Pulmonary Infection. *mBio.* 2019; 10(6). Epub 2019/12/12. <https://doi.org/10.1128/mBio.02759-19> PMID: 31822588; PubMed Central PMCID: PMC6904878.
26. Pulsifer AR, Vashishta A, Reeves SA, Wolfe JK, Palace SG, Proulx MK, et al. Redundant and cooperative roles for *Yersinia pestis* yop effectors in the inhibition of human neutrophil exocytic responses revealed by gain-of-function approach. *Infect Immun.* 2020; 88(3):1–16. <https://doi.org/10.1128/IAI.00909-19> PMID: 31871100
27. Olson RM, Dhariwala MO, Mitchell WJ, Anderson DM. *Yersinia pestis* exploits early activation of MyD88 for growth in the lungs during pneumonic plague. *Infect Immun.* 2019; 87(4). <https://doi.org/10.1128/IAI.00757-18> PMID: 30642901
28. Vagima Y, Zauberan A, Levy Y, Gur D, Tidhar A, Aftalion M, et al. Circumventing *Y. pestis* virulence by early recruitment of neutrophils to the lungs during pneumonic plague. *PLoS Pathog.* 2015; 11(5):e1004893. Epub 2015/05/15. <https://doi.org/10.1371/journal.ppat.1004893> PMID: 25974210; PubMed Central PMCID: PMC4431741.
29. Bennett M, Gilroy DW. Lipid mediators in inflammation. *Microbiol Spectr.* 2016; 4(6). Epub 2016/11/14. <https://doi.org/10.1128/microbiolspec.MCHD-0035-2016> PMID: 27837747.
30. de Paula Rogerio A, Sorgi CA, Sadikot R, Carlo T. The role of lipids mediators in inflammation and resolution. *Biomed Res Int.* 2015; 2015:605959. Epub 2015/04/17. <https://doi.org/10.1155/2015/605959> PMID: 25879029; PubMed Central PMCID: PMC4387946.

31. Afonso PV, Janka-Junttila M, Lee YJ, McCann CP, Oliver CM, Aamer KA, et al. LTB₄ is a signal-relay molecule during neutrophil chemotaxis. *Dev Cell*. 2012; 22(5):1079–91. Epub 2012/05/01. <https://doi.org/10.1016/j.devcel.2012.02.003> PMID: 22542839; PubMed Central PMCID: PMC4141281.
32. Sadik CD, Luster AD. Lipid-cytokine-chemokine cascades orchestrate leukocyte recruitment in inflammation. *J Leukoc Biol*. 2012; 91(2):207–15. Epub 2011/11/08. <https://doi.org/10.1189/jlb.0811402> PMID: 22058421; PubMed Central PMCID: PMC3290425.
33. Peters-Golden M, Henderson WR. Leukotrienes. *The New England Journal of Medicine*. 2007; 357(18). <https://doi.org/10.1056/NEJMra071371> PMID: 17978293
34. Wan M, Tang X, Stsiapanava A, Haeggstrom JZ. Biosynthesis of leukotriene B₄. *Semin Immunol*. 2017; 33:3–15. Epub 2017/10/19. <https://doi.org/10.1016/j.smim.2017.07.012> PMID: 29042025.
35. Crooks SW, Stockley RA. Leukotriene B₄. *The International Journal of Biochemistry and Cell Biology*. 1998; 30(2):173–8. [https://doi.org/10.1016/s1357-2725\(97\)00123-4](https://doi.org/10.1016/s1357-2725(97)00123-4) PMID: 9608670
36. Woo CH, You HJ, Cho SH, Eom YW, Chun JS, Yoo YJ, et al. Leukotriene B₄ stimulates Rac-ERK cascade to generate reactive oxygen species that mediates chemotaxis. *J Biol Chem*. 2002; 277(10):8572–8. Epub 2002/01/05. <https://doi.org/10.1074/jbc.M104766200> PMID: 11756405.
37. Gaudreau R, Le Gouill C, Metaoui S, Lemire S, Stankovaa J, Rola-Pleszczynski M. Signalling through the leukotriene B₄ receptor involves both a_q and a₁₆, but not a_q or a₁₁ G-protein subunits. *Biochem Journal*. 1998; 355(Pt. 1):15–8. <https://doi.org/10.1042/bj3350015> PMID: 9742207
38. Yokomizo T. Two distinct leukotriene B₄ receptors, BLT1 and BLT2. *J Biochem*. 2015; 157(2):65–71. Epub 2014/12/07. <https://doi.org/10.1093/jb/mvu078> PMID: 25480980.
39. He R, Chen Y, Cai Q. The role of the LTB₄-BLT1 axis in health and disease. *Pharmacol Res*. 2020; 158:104857. Epub 2020/05/23. <https://doi.org/10.1016/j.phrs.2020.104857> PMID: 32439596.
40. Powell WS, Rokach J. Biochemistry, biology and chemistry of the 5-lipoxygenase product 5-oxo-EETE. *Prog Lipid Res*. 2005; 44(2–3):154–83. Epub 2005/05/17. <https://doi.org/10.1016/j.plipres.2005.04.002> PMID: 15893379.
41. Radmark O, Samuelsson B. 5-Lipoxygenase: Mechanisms of regulation. *J Lipid Res*. 2009; 50 Suppl (Suppl):S40–5. Epub 2008/11/07. <https://doi.org/10.1194/jlr.R800062-JLR200> PMID: 18987389; PubMed Central PMCID: PMC2674731.
42. Scher JU, Pillinger MH. The anti-inflammatory effects of prostaglandins. *J Investig Med*. 2009; 57(6). <https://doi.org/10.2310/JIM.0b013e31819aaa76> PMID: 19240648
43. Schmid T, Brune B. Prostanoids and resolution of inflammation—Beyond the lipid-mediator class switch. *Front Immunol*. 2021; 12:714042. Epub 2021/07/30. <https://doi.org/10.3389/fimmu.2021.714042> PMID: 34322137; PubMed Central PMCID: PMC8312722.
44. Yokomizo T, Izumi T, Chang K, Takuwa Y, Shimizu T. A G-protein-coupled receptor for leukotriene B₄ that mediates chemotaxis. *Nature*. 1997; 387(6633):620–4. <https://doi.org/10.1038/42506> PMID: 9177352
45. Chaplin DD. Overview of the immune response. *J Allergy Clin Immunol*. 2010; 125(2 Suppl 2):S3–23. Epub 2010/03/05. <https://doi.org/10.1016/j.jaci.2009.12.980> PMID: 20176265; PubMed Central PMCID: PMC2923430.
46. Secatto A, Soares EM, Locachevic GA, Assis PA, Paula-Silva FW, Serezani CH, et al. The leukotriene B₄/BLT₁ axis is a key determinant in susceptibility and resistance to histoplasmosis. *PLoS ONE*. 2014; 9(1):e85083. Epub 2014/01/28. <https://doi.org/10.1371/journal.pone.0085083> PMID: 24465479; PubMed Central PMCID: PMC3897419.
47. Zhang Y, Olson RM, Brown CR. Macrophage LTB₄ drives efficient phagocytosis of *Borrelia burgdorferi* via BLT1 or BLT2. *J Lipid Res*. 2017; 58(3):494–503. Epub 2017/01/06. <https://doi.org/10.1194/jlr.M068882> PMID: 28053185; PubMed Central PMCID: PMC5335579.
48. Sun Y, Connor MG, Pennington JM, Lawrenz MB. Development of bioluminescent bioreporters for *in vitro* and *in vivo* tracking of *Yersinia pestis*. *PLoS ONE*. 2012; 7(10):e47123. Epub 2012/10/17. <https://doi.org/10.1371/journal.pone.0047123> PMID: 23071730; PubMed Central PMCID: PMC3469486.
49. Haribabu B, Verghese MW, Steeber DA, Sellars DD, Bock CB, Snyderman R. Targeted disruption of the leukotriene B₄ receptor in mice reveals its role in inflammation and platelet-activating factor-induced anaphylaxis. *J Exp Med*. 2000; 192(3). <https://doi.org/10.1084/jem.192.3.433> PMID: 10934231
50. Palace SG, Proulx MK, Szabady RL, Goguen JD. Gain-of-function analysis reveals important virulence roles for the *Yersinia pestis* type III secretion system effectors YopJ, YopT, and YpkA. *Infect Immun*. 2018; 86(9):1–11. <https://doi.org/10.1128/IAI>
51. Auerbuch V, Golenbock DT, Isberg RR. Innate immune recognition of *Yersinia pseudotuberculosis* type III secretion. *PLoS Pathog*. 2009; 5(12):e1000686. Epub 2009/12/10. <https://doi.org/10.1371/journal.ppat.1000686> PMID: 19997504; PubMed Central PMCID: PMC2779593.

52. Chung LK, Bliska JB. *Yersinia* versus host immunity: how a pathogen evades or triggers a protective response. *Curr Opin Microbiol*. 2016; 29:56–62. Epub 2015/12/08. <https://doi.org/10.1016/j.mib.2015.11.001> PMID: 26638030; PubMed Central PMCID: PMC4755919.
53. Zwack EE, Snyder AG, Wynosky-Dolfi MA, Ruthel G, Philip NH, Marketon MM, et al. Inflammasome activation in response to the *Yersinia* type III secretion system requires hyperinjection of translocon proteins YopB and YopD. *mBio*. 2015; 6(1):e02095–14. Epub 2015/02/19. <https://doi.org/10.1128/mBio.02095-14> PMID: 25691590; PubMed Central PMCID: PMC4337566.
54. Brodsky IE, Palm NW, Sadanand S, Ryndak MB, Sutterwala FS, Flavell RA, et al. A *Yersinia* effector protein promotes virulence by preventing inflammasome recognition of the type III secretion system. *Cell Host Microbe*. 2010; 7(5):376–87. Epub 2010/05/19. <https://doi.org/10.1016/j.chom.2010.04.009> PMID: 20478539; PubMed Central PMCID: PMC2883865.
55. Davis AJ, Meccas J. Mutations in the *Yersinia pseudotuberculosis* type III secretion system needle protein, YscF, that specifically abrogate effector translocation into host cells. *J Bacteriol*. 2007; 189(1):83–97. Epub 2006/10/27. <https://doi.org/10.1128/JB.01396-06> PMID: 17071752; PubMed Central PMCID: PMC1797200.
56. Kwuan L, Adams W, Auerbuch V. Impact of host membrane pore formation by the *Yersinia pseudotuberculosis* type III secretion system on the macrophage innate immune response. *Infect Immun*. 2013; 81(3):905–14. Epub 2013/01/07. <https://doi.org/10.1128/IAI.01014-12> PMID: 23297383; PubMed Central PMCID: PMC3584892.
57. Hegde B, Bodduluri SR, Satpathy SR, Alghsham RS, Jala VR, Uriarte SM, et al. Inflammasome-independent leukotriene B₄ production drives crystalline silica-induced sterile inflammation. *J Immunol*. 2018; 200(10):3556–67. Epub 2018/04/04. <https://doi.org/10.4049/jimmunol.1701504> PMID: 29610142; PubMed Central PMCID: PMC5940517.
58. Satpathy SR, Jala VR, Bodduluri SR, Krishnan E, Hegde B, Hoyle GW, et al. Crystalline silica-induced leukotriene B₄-dependent inflammation promotes lung tumour growth. *Nat Commun*. 2015; 6:7064. Epub 2015/04/30. <https://doi.org/10.1038/ncomms8064> PMID: 25923988; PubMed Central PMCID: PMC4418220.
59. Sorgi CA, Rose S, Court N, Carlos D, Paula-Silva FW, Assis PA, et al. GM-CSF priming drives bone marrow-derived macrophages to a pro-inflammatory pattern and downmodulates PGE₂ in response to TLR2 ligands. *PLoS ONE*. 2012; 7(7):e40523. Epub 2012/07/19. <https://doi.org/10.1371/journal.pone.0040523> PMID: 22808181; PubMed Central PMCID: PMC3396658.
60. Lacey DC, Achuthan A, Fleetwood AJ, Dinh H, Roiniotis J, Scholz GM, et al. Defining GM-CSF- and macrophage-CSF-dependent macrophage responses by *in vitro* models. *J Immunol*. 2012; 188(11):5752–65. Epub 2012/05/02. <https://doi.org/10.4049/jimmunol.1103426> PMID: 22547697.
61. Serezani CH, Divangahi M, Peters-Golden M. Leukotrienes in innate immunity: still underappreciated after all these years? *J Immunol*. 2023; 210(3):221–7. Epub 2023/01/18. <https://doi.org/10.4049/jimmunol.2200599> PMID: 36649580.
62. Peters-Golden M, Canetti C, Mancuso P, Coffey MJ. Leukotrienes: Underappreciated mediators of innate immune responses. *J Immunol*. 2005; 174(2):589–94. Epub 2005/01/07. <https://doi.org/10.4049/jimmunol.174.2.589> PMID: 15634873.
63. Subramanian BC, Moissoglu K, Parent CA. The LTB₄-BLT1 axis regulates the polarized trafficking of chemoattractant GPCRs during neutrophil chemotaxis. *J Cell Sci*. 2018; 131(18). Epub 2018/08/31. <https://doi.org/10.1242/jcs.217422> PMID: 30158177; PubMed Central PMCID: PMC6176921.
64. Kwak DW, Park D, Kim JH. Leukotriene B₄ receptors are necessary for the stimulation of NLRP3 inflammasome and IL-1β synthesis in neutrophil-dominant asthmatic airway inflammation. *Biomedicines*. 2021; 9(5). Epub 2021/06/03. <https://doi.org/10.3390/biomedicines9050535> PMID: 34064821; PubMed Central PMCID: PMC8151312.
65. Lammermann T, Afonso PV, Angermann BR, Wang JM, Kastnermuller W, Parent CA, et al. Neutrophil swarms require LTB₄ and integrins at sites of cell death *in vivo*. *Nature*. 2013; 498(7454):371–5. Epub 2013/05/28. <https://doi.org/10.1038/nature12175> PMID: 23708969; PubMed Central PMCID: PMC3879961.
66. McDonald PP, McColl SR, Braquet P, Borgeat P. Autocrine enhancement of leukotriene synthesis by endogenous leukotriene B₄ and platelet-activating factor in human neutrophils. *Br J Pharmacol*. 1994; 111(3). <https://doi.org/10.1111/j.1476-5381.1994.tb14816.x> PMID: 8019762
67. Irimia D. Neutrophil swarms are more than the accumulation of cells. *Microbiol Insights*. 2020; 13:1178636120978272. Epub 2020/12/24. <https://doi.org/10.1177/1178636120978272> PMID: 33354109; PubMed Central PMCID: PMC7734531.
68. Poplimont H, Georgantzoglou A, Boulch M, Walker HA, Coombs C, Papaleonidopoulou F, et al. Neutrophil swarming in damaged tissue is orchestrated by connexins and cooperative calcium alarm

- signals. *Curr Biol*. 2020; 30(14):2761–76 e7. Epub 2020/06/06. <https://doi.org/10.1016/j.cub.2020.05.030> PMID: 32502410; PubMed Central PMCID: PMC7372224.
69. Shannon JG, Hasenkrug AM, Dorward DW, Nair V, Carmody AB, Hinnebusch BJ. *Yersinia pestis* subverts the dermal neutrophil response in a mouse model of bubonic plague. *mBio*. 2013; 4(5):e00170–13. Epub 2013/08/29. <https://doi.org/10.1128/mBio.00170-13> PMID: 23982068; PubMed Central PMCID: PMC3760243.
 70. Kienle K, Glaser KM, Eickhoff S, Mihlan M, Knopper K, Reategui E, et al. Neutrophils self-limit swarming to contain bacterial growth *in vivo*. *Science*. 2021; 372(6548). Epub 2021/06/19. <https://doi.org/10.1126/science.abe7729> PMID: 34140358; PubMed Central PMCID: PMC8926156.
 71. Kienle K, Lammermann T. Neutrophil swarming: an essential process of the neutrophil tissue response. *Immunol Rev*. 2016; 273(1):76–93. Epub 2016/08/26. <https://doi.org/10.1111/imr.12458> PMID: 27558329.
 72. Chou RC, Kim ND, Sadik CD, Seung E, Lan Y, Byrne MH, et al. Lipid-cytokine-chemokine cascade drives neutrophil recruitment in a murine model of inflammatory arthritis. *Immunity*. 2010; 33(2):266–78. Epub 2010/08/24. <https://doi.org/10.1016/j.immuni.2010.07.018> PMID: 20727790; PubMed Central PMCID: PMC3155777.
 73. Bliska JB, Wang X, Viboud GI, Brodsky IE. Modulation of innate immune responses by *Yersinia* type III secretion system translocators and effectors. *Cell Microbiol*. 2013; 15(10):1622–31. Epub 2013/07/10. <https://doi.org/10.1111/cmi.12164> PMID: 23834311; PubMed Central PMCID: PMC3788085.
 74. Oh C, Li L, Verma A, Reuven AD, Miao EA, Bliska JB, et al. Neutrophil inflammasomes sense the subcellular delivery route of translocated bacterial effectors and toxins. *Cell Rep*. 2022; 41(8):111688. <https://doi.org/10.1016/j.celrep.2022.111688> PMID: 36417874; PubMed Central PMCID: PMC9827617.
 75. Chen KW, Demarco B, Ramos S, Heilig R, Goris M, Graczyk JP, et al. RIPK1 activates distinct gasdermins in macrophages and neutrophils upon pathogen blockade of innate immune signaling. *Proc Natl Acad Sci U S A*. 2021; 118(28). <https://doi.org/10.1073/pnas.2101189118> PMID: 34260403; PubMed Central PMCID: PMC8285957.
 76. Chung LK, Park YH, Zheng Y, Brodsky IE, Hearing P, Kastner DL, et al. The *Yersinia* virulence factor YopM hijacks host kinases to inhibit type III effector-triggered activation of the pyrin inflammasome. *Cell Host Microbe*. 2016; 20(3):296–306. Epub 2016/08/30. <https://doi.org/10.1016/j.chom.2016.07.018> PMID: 27569559; PubMed Central PMCID: PMC5025386.
 77. von Moltke J, Trinidad NJ, Moayeri M, Kintzer AF, Wang SB, van Rooijen N, et al. Rapid induction of inflammatory lipid mediators by the inflammasome *in vivo*. *Nature*. 2012; 490(7418):107–11. Epub 2012/08/21. <https://doi.org/10.1038/nature11351> PMID: 22902502; PubMed Central PMCID: PMC3465483.
 78. Zoccal KF, Sorgi CA, Hori JI, Paula-Silva FW, Arantes EC, Serezani CH, et al. Opposing roles of LTB₄ and PGE₂ in regulating the inflammasome-dependent scorpion venom-induced mortality. *Nat Commun*. 2016; 7:10760. Epub 2016/02/26. <https://doi.org/10.1038/ncomms10760> PMID: 26907476; PubMed Central PMCID: PMC4766425.
 79. Yokomizo T, Izumi T, Shimizu T. Leukotriene B₄: metabolism and signal transduction. *Arch Biochem Biophys*. 2001; 385(2):231–41. Epub 2001/05/23. <https://doi.org/10.1006/abbi.2000.2168> PMID: 11368003.
 80. Palmer LE, Hobbie S, Galan JE, Bliska JB. YopJ of *Yersinia pseudotuberculosis* is required for the inhibition of macrophage TNF- α production and downregulation of the MAP kinases p38 and JNK. *Mol Microbiol*. 1998; 27(5):953–65.
 81. Grabowski B, Schmidt MA, Ruter C. Immunomodulatory *Yersinia* outer proteins (Yops)—useful tools for bacteria and humans alike. *Virulence*. 2017; 8(7):1124–47. Epub 2017/03/16. <https://doi.org/10.1080/21505594.2017.1303588> PMID: 28296562; PubMed Central PMCID: PMC5711447.
 82. Viboud GI, Mejia E, Bliska JB. Comparison of YopE and YopT activities in counteracting host signalling responses to *Yersinia pseudotuberculosis* infection. *Cell Microbiol*. 2006; 8(9):1504–15. <https://doi.org/10.1111/j.1462-5822.2006.00729.x> PMID: 16922868.
 83. Andersson K, Magnusson K, Majeed M, Stendahl O, Fallman M. *Yersinia pseudotuberculosis*-Induced Calcium Signaling in Neutrophils Is Blocked by the Virulence Effector YopH. *Infect Immun*. 1999; 67(5). <https://doi.org/10.1128/IAI.67.5.2567-2574.1999> PMID: 10225922
 84. Pha K, Wright ME, Barr TM, Eigenheer RA, Navarro L. Regulation of *Yersinia* protein kinase A (YpkA) kinase activity by multisite autophosphorylation and identification of an N-terminal substrate-binding domain in YpkA. *J Biol Chem*. 2014; 289(38):26167–77. Epub 2014/08/01. <https://doi.org/10.1074/jbc.M114.601153> PMID: 25086045; PubMed Central PMCID: PMC4176208.

85. Viboud GI, Bliska JB. *Yersinia* outer proteins: role in modulation of host cell signaling responses and pathogenesis. *Annu Rev Microbiol*. 2005; 59:69–89. Epub 2005/04/26. <https://doi.org/10.1146/annurev.micro.59.030804.121320> PMID: 15847602.
86. Aepfelbacher M, Trasak C, Ruckdeschel K. Effector functions of pathogenic *Yersinia* species. *Thromb Haemost*. 2007; 98(09):521–9. <https://doi.org/10.1160/th07-03-0173>
87. Eruslanov EB, Singhal S, Albelda SM. Mouse versus human neutrophils in cancer: a major knowledge gap. *Trends Cancer*. 2017; 3(2):149–60. Epub 2017/07/19. <https://doi.org/10.1016/j.trecan.2016.12.006> PMID: 28718445; PubMed Central PMCID: PMC5518602.
88. Mestas J, Hughes CC. Of mice and not men: differences between mouse and human immunology. *J Immunol*. 2004; 172(5):2731–8. Epub 2004/02/24. <https://doi.org/10.4049/jimmunol.172.5.2731> PMID: 14978070.
89. Shay T, Jojic V, Zuk O, Rothamel K, Puyraimond-Zemmour D, Feng T, et al. Conservation and divergence in the transcriptional programs of the human and mouse immune systems. *Proc Natl Acad Sci U S A*. 2013; 110(8):2946–51. Epub 2013/02/06. <https://doi.org/10.1073/pnas.1222738110> PMID: 23382184; PubMed Central PMCID: PMC3581886.
90. Zheng Y, Sefik E, Astle J, Karatepe K, Oz HH, Solis AG, et al. Human neutrophil development and functionality are enabled in a humanized mouse model. *Proc Natl Acad Sci U S A*. 2022; 119(43): e2121077119. Epub 2022/10/22. <https://doi.org/10.1073/pnas.2121077119> PMID: 36269862; PubMed Central PMCID: PMC9618085.
91. Zschaler J, Schlorke D, Arnhold J. Differences in innate immune response between man and mouse. *Crit Rev Immunol*. 2014. <https://doi.org/10.1615/CritRevImmunol.2014011600> PMID: 25404048
92. Maddipati KR. Non-inflammatory physiology of “inflammatory” mediators—*unalamation*, a new paradigm. *Front Immunol*. 2020; 11:580117. Epub 2020/10/30. <https://doi.org/10.3389/fimmu.2020.580117> PMID: 33117385; PubMed Central PMCID: PMC7575772.
93. Murakami Y, Akahoshi T, Hayashi I, Endo H, Hashimoto A, Kono S, et al. Inhibition of monosodium urate monohydrate crystal-induced acute inflammation by retrovirally transfected prostaglandin D synthase. *Arthritis Rheum*. 2003; 48(10):2931–41. Epub 2003/10/15. <https://doi.org/10.1002/art.11271> PMID: 14558100.
94. Storer PD, Xu J, Chavis JA, Drew PD. Cyclopentenone prostaglandins PGA₂ and 15-deoxy-D^{12,14} PGJ₂ suppress activation of murine microglia and astrocytes: implications for multiple sclerosis. *J Neurosci Res*. 2005; 80(1):66–74. Epub 2005/02/22. <https://doi.org/10.1002/jnr.20413> PMID: 15723383; PubMed Central PMCID: PMC2819749.
95. Loynes CA, Lee JA, Robertson AL, Steel MJ, Ellett F, Feng Y, et al. PGE₂ production at sites of tissue injury promotes an anti-inflammatory neutrophil phenotype and determines the outcome of inflammation resolution *in vivo*. *Science Advances*. 2018; 4(9):eaar8320. <https://doi.org/10.1126/sciadv.aar8320> PMID: 30191175
96. Serezani CH, Chung J, Ballinger MN, Moore BB, Aronoff DM, Peters-Golden M. Prostaglandin E₂ suppresses bacterial killing in alveolar macrophages by inhibiting NADPH oxidase. *Am J Respir Cell Mol Biol*. 2007; 37(5):562–70. Epub 2007/06/23. <https://doi.org/10.1165/rcmb.2007-0153OC> PMID: 17585108; PubMed Central PMCID: PMC2048683.
97. Aronoff DM, Canetti C, Serezani CH, Luo M, Peters-Golden M. Cutting edge: macrophage inhibition by cyclic AMP (cAMP): differential roles of protein kinase A and exchange protein directly activated by cAMP-1. *J Immunol*. 2005; 174(2):595–9. Epub 2005/01/07. <https://doi.org/10.4049/jimmunol.174.2.595> PMID: 15634874.
98. Lee SP, Serezani CH, Medeiros AI, Ballinger MN, Peters-Golden M. Crosstalk between prostaglandin E₂ and leukotriene B₄ regulates phagocytosis in alveolar macrophages via combinatorial effects on cyclic AMP. *J Immunol*. 2009; 182(1):530–7. Epub 2008/12/26. <https://doi.org/10.4049/jimmunol.182.1.530> PMID: 19109185.
99. Luo M, Jones SM, Phare SM, Coffey MJ, Peters-Golden M, Brock TG. Protein kinase A inhibits leukotriene synthesis by phosphorylation of 5-lipoxygenase on serine 523. *J Biol Chem*. 2004; 279(40):41512–20. Epub 2004/07/29. <https://doi.org/10.1074/jbc.M312568200> PMID: 15280375.
100. Price SL, Vadyvaloo V, DeMarco JK, Brady A, Gray PA, Kehl-Fie TE, et al. Yersiniabactin contributes to overcoming zinc restriction during *Yersinia pestis* infection of mammalian and insect hosts. *Proc Natl Acad Sci U S A*. 2021; 118(44). Epub 2021/10/31. <https://doi.org/10.1073/pnas.2104073118> PMID: 34716262; PubMed Central PMCID: PMC8612365.
101. Calderin EP, Zheng J-J, Boyd NL, McNally L, Audam TN, Lorkiewicz P, et al. Exercise-induced specialized proresolving mediators stimulate AMPK phosphorylation to promote mitochondrial respiration in macrophages. *Molecular Metabolism*. 2022; 66:101637. <https://doi.org/10.1016/j.molmet.2022.101637> PMID: 36400404

102. Maddipati KR, Zhou SL. Stability and analysis of eicosanoids and docosanoids in tissue culture media. *Prostaglandins Other Lipid Mediat.* 2011; 94(1–2):59–72. Epub 2011/01/18. <https://doi.org/10.1016/j.prostaglandins.2011.01.003> PMID: 21236355.
103. Maddipati KR, Romero R, Chaiworapongsa T, Chaemsaitong P, Zhou SL, Xu Z, et al. Lipidomic analysis of patients with microbial invasion of the amniotic cavity reveals up-regulation of leukotriene B4. *FASEB J.* 2016; 30(10):3296–307. Epub 2016/06/18. <https://doi.org/10.1096/fj.201600583R> PMID: 27312808; PubMed Central PMCID: PMC5024690.
104. Maddipati KR, Romero R, Chaiworapongsa T, Chaemsaitong P, Zhou SL, Xu Z, et al. Clinical chorioamnionitis at term: the amniotic fluid fatty acyl lipidome. *J Lipid Res.* 2016; 57(10):1906–16. Epub 2016/08/20. <https://doi.org/10.1194/jlr.P069096> PMID: 27538821; PubMed Central PMCID: PMC5036371.
105. Haslett C, Guthrie LA, Kopaniak MM, Johnston RB Jr, Henson PM. Modulation of multiple neutrophil functions by preparative methods or trace concentrations of bacterial lipopolysaccharide. *Am J Pathol.* 1985;119. PMID: 2984939
106. Werz O, Gerstmeier J, Libreros S, De la Rosa X, Werner M, Norris PC, et al. Human macrophages differentially produce specific resolvin or leukotriene signals that depend on bacterial pathogenicity. *Nat Commun.* 2018; 9(1):59. Epub 2018/01/06. <https://doi.org/10.1038/s41467-017-02538-5> PMID: 29302056; PubMed Central PMCID: PMC5754355.
107. Li Q, Anderson CD, Egilmez NK. Inhaled IL-10 suppresses lung tumorigenesis via abrogation of inflammatory macrophage-Th17 cell axis. *J Immunol.* 2018; 201(9):2842–50. Epub 2018/09/28. <https://doi.org/10.4049/jimmunol.1800141> PMID: 30257887.
108. Bodduluri SR, Mathis S, Maturu P, Krishnan E, Satpathy SR, Chilton PM, et al. Mast cell-dependent CD8⁺ T-cell recruitment mediates immune surveillance of intestinal tumors in *Apc*^{Min/+} mice. *Cancer Immunol Res.* 2018; 6(3):332–47. Epub 2018/02/01. <https://doi.org/10.1158/2326-6066.CIR-17-0424> PMID: 29382671; PubMed Central PMCID: PMC9580996.
109. Schindelin J, Arganda-Carreras I, Frise E, Kaynig V, Longair M, Pietzsch T, et al. Fiji: an open-source platform for biological-image analysis. *Nat Methods.* 2012; 9(7):676–82. Epub 2012/06/30. <https://doi.org/10.1038/nmeth.2019> PMID: 22743772; PubMed Central PMCID: PMC3855844.
110. Jin J, Wahlang B, Thapa M, Head KZ, Hardesty JE, Srivastava S, et al. Proteomics and metabolic phenotyping define principal roles for the aryl hydrocarbon receptor in mouse liver. *Acta Pharm Sin B.* 2021; 11(12):3806–19. Epub 2022/01/14. <https://doi.org/10.1016/j.apsb.2021.10.014> PMID: 35024308; PubMed Central PMCID: PMC8727924.
111. Srivastava S, Merchant M, Rai A, Rai SN. Standardizing proteomics workflow for liquid chromatography-mass spectrometry: Technical and statistical considerations. *J Proteomics Bioinform.* 2019; 12(3):48–55. Epub 2019/01/01. <https://doi.org/10.35248/0974-276x.19.12.496> PMID: 32148359; PubMed Central PMCID: PMC7059694.
112. Srivastava S, Merchant M, McClain CJ, Rai A, Chaturvedi KK, Angadi UB, et al. Advanced multivariable statistical analysis interactive tool for handling missing data and confounding covariates for label-free LC-MS proteomics experiments. *Current Bioinformatics.* 2023; 18(2). <https://doi.org/10.2174/1574893618666230223150253>